Periodico di Mineralogia (2012), 81, 2, 179-204 DOI: 10.2451/2012PM0011

PERIODICO di MINERALOGIA
established in 1930

An International Journal of
MINERALOGY, CRYSTALLOGRAPHY, GEOCHEMISTRY,
ORE DEPOSITS, PETROLOGY, VOLCANOLOGY
and applied topics on *Environment*, *Archeometry* and *Cultural Heritage*

A volcano-sedimentary sequence with albitite layers in the Variscan basement of NE Sardinia: a petrographical and geochemical study

Luca G. Costamagna[1], Gabriele Cruciani[1,*], Marcello Franceschelli[1] and Mariano Puxeddu[2]

[1]Dipartimento di Scienze Chimiche e Geologiche, Università di Cagliari, Via Trentino, 51 - 09127 Cagliari (Italy)
[2]Former researcher of the Istituto di Geoscienze e Georisorse CNR-Pisa, Via Moruzzi, 1 - 56124 Pisa (Italy)
[*]Corresponding author: *gcrucian@unica.it*

Abstract

A metamorphosed volcanoclastic-sedimentary succession has been discovered near the village of Lula, in NE Sardinia with the following main lithotypes from bottom to top: 1) metavolcanics; 2) yellowish metasandstones; 3) greenish to grey metapsammopelites. The metavolcanics, of dacitic/andesitic composition, and with variable modal amounts (10-40%) of albite phenocrysts, include two albitite layers. The yellowish metasandstones form sequences with basal microconglomerates, passing upwards with a wavy erosional surface to the overlying metasiltite-metapelite sequence. The greenish to grey metapsammopelites mainly consist of alternating albite-rich phyllites and dark phyllites. The Lula metavolcanics show REE patterns similar to those of the Ordovician metavolcanics from Gerrei, Sarcidano and Sarrabus. NMORB normalised trace element patterns with negative Nb and Ta anomalies demonstrate the calcalkaline affinity of the Lula metavolcanics. The albitite layers consist of up to 90-95 modal percent albite and up to 9 wt.% Na_2O. Rocks with this unusual composition could have been generated only by hydrothermal fluids associated with the Ordovician volcanism or to the final cooling stages of a calcalkaline pre-Variscan intrusive body. The K_2O, Na_2O, SiO_2 and Al_2O_3 contents reveal that the yellowish metasandstones plot in the fields of greywackes or pelitic greywackes, the greenish to grey metapsammopelites in the fields of pelites or pelitic greywackes.

Compared to the metapsammopelites, the metasandstones reveal slightly higher SiO_2, Zr and Hf contents, significant Na_2O enrichment, slightly lower Al_2O_3, Fe_2O_3, Ba, Rb and Cs contents and strong K_2O depletion. The greenish to grey metapsammopelites show chondrite normalised REE patterns almost identical to those of the Ordovician metavolcanics and similar to those of North American Shale Composite and Post Archaean Australian Shale. The shallow metavolcanic succession is probably made up of primary volcanic products and/or deposits of their reworked detrital materials. Thin, discontinuous dark metapelitic layers in the metavolcanic succession are actually sedimentary layers marking short quiescence periods in volcanic activity. The protoliths of the metasedimentary rocks were shallow marine sediments.

The protoliths of the yellowish metasandstones may be attributed to mid- to high-energy environments while those of the metapsammopelites indicate alternating mid- to low-energy environments. In the yellowish metasandstones 45 microsequences have been identified. They show thickening-to-thinning-upwards sedimentary trends that may be interpreted as a backward to forward migration of the sequences with respect to the shoreline resulting in an increase or decrease of depositional energy, respectively. All the rocks were metamorphosed and multideformed during the Variscan orogeny. The P-T conditions of a biotite-bearing metasandstone have been estimated at T = 430-470 °C, P = 0.65-0.95 GPa by P-T pseudosection modelling.

Key words: volcano-sedimentary sequence; albitite layers; petrography; geochemistry; Variscan Sardinia.

Introduction

A geo-petrographic survey of Variscan metamorphic rocks south of the village of Lula in NE Sardinia revealed the existence of a volcano-sedimentary sequence, including two centimetre- thick intercalations of almost pure albitite layers. These intriguing layers consist almost entirely of albite, as indicated by a modal abundance of more than 90% and a Na_2O content of about 9 wt.%. In the northern segment of the Sardinian Variscan belt, Helbing (2003) discovered the occurrence of a metamorphic sequence named by him the "Orune schists", composed of alternating porphyroids, greenschists, graphitic schists and metapsammopelites. They should be roughly correlated with the intermediate to acidic volcano-sedimentary sequences of the Ordovician to Devonian-Early Carboniferous tectono-sedimentary Variscan cycle of Central and Southern Sardinia, including the Ordovician calcalkaline suite (Memmi et al., 1983).

In this paper a detailed geochemical and petrographical study has been conducted in an attempt to identify the source rocks for both sedimentary and volcanoclastic materials. Further, the relict sedimentary structures and the geochemistry of the investigated rocks provided indications of the local lithostratigraphy and the original depositional environments. Comparison with the igneous-sedimentary successions in the northern and southern segments of the Variscan belt in Sardinia will enable us to fit the tessera of the Lula sequence into its right place in the Variscan mosaic of NE Sardinia.

Geological setting

Four tectono-metamorphic zones can be distinguished within the Sardinian segment of the Variscan belt (Carmignani et al., 2001, and references therein). From SW to NE they are: 1) External Zone (southern Sardinia, Iglesiente-Sulcis), 2) External Nappe Zone (central to southern Sardinia), 3) Internal Nappe Zone (northern to central Sardinia), 4) Inner or Axial Zone (northern Sardinia). The External Zone is featured at the bottom by an Early Cambrian to Early Ordovician shelf shallow succession made of siliciclastic to carbonate deposits (Bechstadt and Boni, 1994, and references therein). It is followed unconformably (Sardic Phase) by a siliciclastic, gradually deepening succession (Leone et al., 1991) from Late Ordovician to Early Carboniferous in age. Volcanic contributions are very scarce and present only in the Late Ordovician units: they are essentially reworked deposits. Metamorphism in the External Zone is very low.

A thick volcano-sedimentary to epiclastic succession of Middle to Late Ordovician age is present mainly in the External Nappe Zone. Here the Lower Middle Ordovician volcano-sedimentary complex (metalavas, metapyroclastics, metaepiclastics, metasandstones, metasiltites) of calcalkaline affinity corresponds roughly to the Fm. di Monte Santa Vittoria (Pertusati et al., 2002). This unit rests over the Conglomerati di Muravera (Carmignani et al., 2002) that marks the Sarrabese unconformity (Middle Ordovician, Calvino et al., 1958) and cover unconformably the Fm. delle Arenarie di San Vito. The Fm. di Santa Vittoria is followed by a Late Ordovician fining upward, continental to marine siliciclastic unit starting from epiclastic, arkosic deposits bounded to the dismantling of Ordovician volcanic arc and passing to pelitic, fine dark deposits of confined platform referable to the black shales facies.

The main lithotypes in the Internal Nappe Zone are: metasandstones, quartzites and phyllites outcropping in the Monti del Gennargentu, central Sardinia ("Postgotlandiano" Auct. p.p.), metaconglomerates, micaschists and paragneisses, acidic metavolcanic rocks ("Porfiroidi"), associated with metarkoses and microcline-bearing quartzites, and mafic to intermediate (andesite) metavolcanic rocks of likely Middle-Ordovician age. The Ordovician volcano-sedimentary to epiclastic sequence forms only small scattered outcrops in this zone (Oggiano et al., 2010). More recent sequences include Siluro-Devonian graphite-rich phyllites, marble and calcschist intercalations and metadolerites and metagabbros. The thickness of the entire succession is supposed to be around 1000-1200 m.

The Axial Zone comprises two metamorphic complexes: the Low to Medium Grade Metamorphic Complex (L-MGMC) made up of micaschists, paragneisses and orthogneisses with a metamorphic grade up to amphibolite-facies and the High Grade Metamorphic Complex (HGMC) mainly consisting of igneous- and sedimentary-derived migmatites with lenses of retrogressed granulites and eclogites (Franceschelli et al., 1982; 2005). The two metamorphic complexes are separated by the Posada-Asinara tectonic Line (Elter et al., 1990; 1999) interpreted by Helbing and Tiepolo (2005), Giacomini et al. (2005) and Padovano et al. (2012) as a major late Variscan sinistral shear line involving parts of the same Gondwana domain. The studied volcano-sedimentary sequence outcrops south of Lula village, in the northernmost areas of the Internal Nappe Zone near the southern border of the Axial Zone (Figure 1). Metamorphic zoning of pelitic and quartz-feldspathic sequences in the Lula area, based on the regional distribution of AFM minerals, consists from South to North of a classic Barrovian zonal sequence from biotite to sillimanite zone (Franceschelli et al., 1982; 1989). Many estimates of metamorphic temperature and pressure are reported for rocks of the NE Sardinian basement (Franceschelli et al., 1982; 1989; Carosi and Palmeri, 2002). The P-T time path for NE Sardinian rocks is clockwise, typical of continental collision. It involves an early stage that is prograde with respect to temperature and pressure up to the pressure peak, followed by a stage with increasing temperature and falling pressure. Peak temperature was reached later than peak pressure (Franceschelli et al., 1982). In the deeper garnet zone, P of about 1.0 GPa and T near 450 °C have been estimated for the D_1 stage. A later pressure decrease of 0.2-0.3 GPa and a temperature increase of about 40-50 °C, up to T ~ 500 °C led to peak metamorphic P-T conditions (Franceschelli et al., 1982). However, no P-T estimates are so far available for the rocks pertaining to the biotite zone.

Carmignani et al. (1982) and Elter et al. (1986) distinguished three main deformation phases in the Lula area (D_1, D_2, D_3). The D_1 phase is characterised by southward recumbent isoclinal folds with penetrative axial plane schistosity S_1. The D_2 phase produced folds with E-W trending

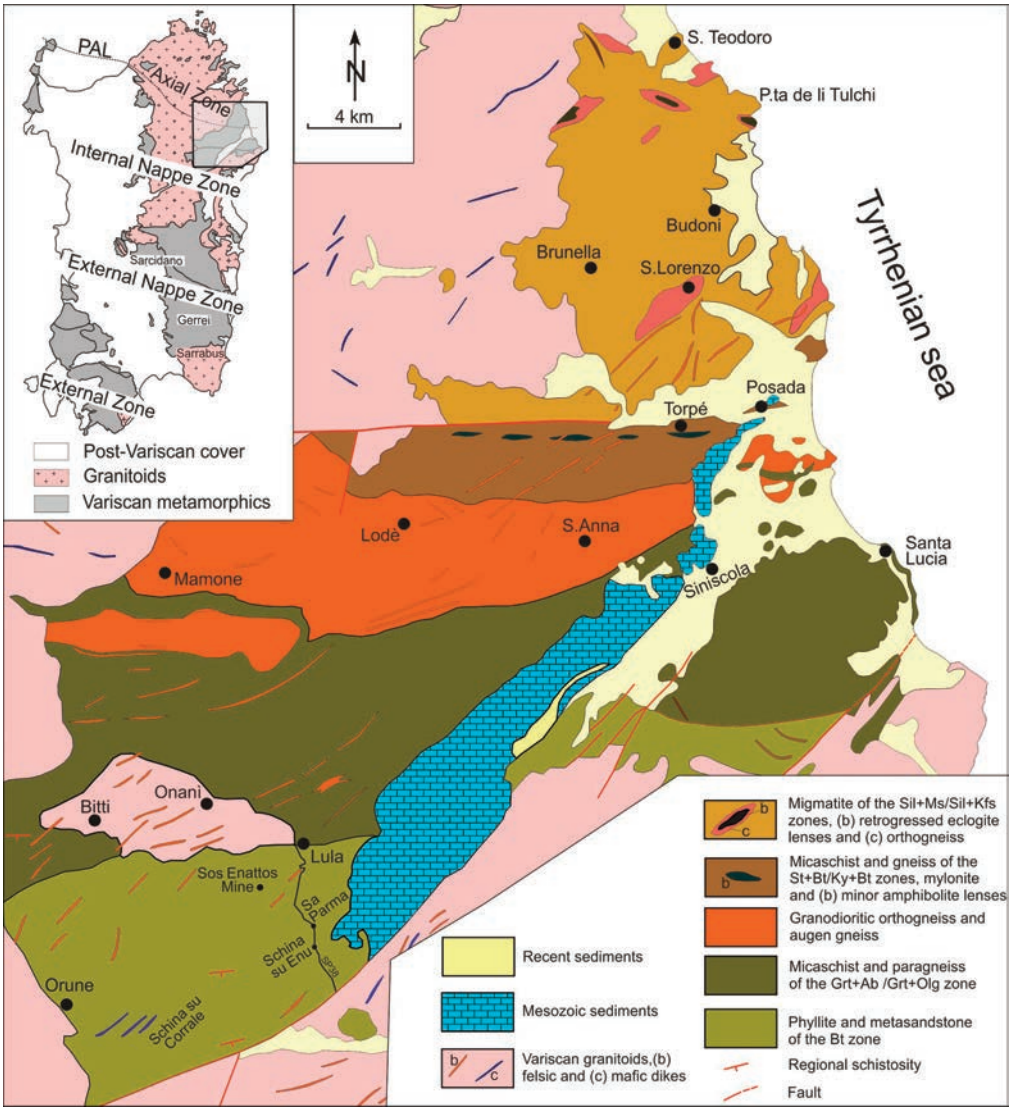

Figure 1. Geological sketch map of NE Sardinia modified from the 1:200 000 geological map of Sardinia, northern sheet. The insert shows the simplified tectonic sketch map of the Variscan belt in Sardinia, modified from Carmignani et al. (2001).

axes. D_2 folds are open and characterised by strain-slip S_2 schistosity. Moving northwards, D_2 folds turn into tight northward recumbent isoclinal folds with a southward dipping S_2 schistosity that almost completely obliterated the D_1 structural features. The D_3 phase generated chevron, box or kink folds, with N-S trending axes locally associated with strain-slip or fracture cleavage. Elter in Oggiano and Di Pisa (1992) proposed two more deformation phases

(D_4, D_5). The D_4 phase generated a mylonitic complex with continuous gradual transition from an S-C structure to an ultramylonitic one whereas the D_5 phase produced a kilometre-wide flexure with sub-horizontal axis parallel to the orogenic trend (Helbing, 2003). Di Vincenzo et al. (2004) in the micaschist of the garnet zone report in situ ^{40}Ar-^{39}Ar ages of ~ 340 Ma for syn-S_1 phengite and of ~ 320 Ma for syn-S_2 white mica. All the Variscan units were intruded by Carboniferous-Permian granitoids.

Field geology

A geo-petrographic survey of the metamorphic succession cropping out south of Lula was conducted along the SP38 road from Schina Su Enu to Sa Parma (Figure 1). Owing to the major shortening produced by the Variscan deformation it is very difficult to reconstruct the stratigraphy, as well as the thickness of the different units and of the succession as a whole. The main N40°-50° striking, SE-dipping S_2 schistosity in the pelitic rocks lies almost parallel to the S_0 bedding plane. S_1 schistosity is always recognizable at the microscopic scale. In the metasandstones S_1 is the main schistosity and S_2 is clearly detectable in the fold hinges. The main lithological groups of the studied succession can be schematised as follows, from bottom to top: metavolcanics, yellowish metasandstones, greenish to grey metasedimentary group.

The metavolcanics show variable modal amounts (10-40 %) of relict igneous plagioclase crystals and of phyllosilicates. Quartz is abundant. The subrounded to elliptical shape of these phenocrysts suggests partial reworking and limited transport. The best preserved outcrop can be observed at Schina su Enu (Figure 2). From bottom to top, the Schina su Enu sequence consists of the following nine layers:

Layer A: whitish albite crystals up to 4-5 mm in size flattened parallel to the main schistosity are embedded in a fine-grained brownish matrix. Submillimetre-sized biotite and white mica blades, sometimes in glomeroporphyritic assemblages, are visible to the naked eye. The estimated thickness of this layer, partly covered by debris, is about a few decimetres.

Layer B: very fine-grained whitish albitite layer with a maximum thickness of about 8-10 cm, shows a faint schistosity outlined by thin black biotite trails.

Layer C: 8-10 cm-thick brownish layer very similar to layer A. It shows elongated, millimetre-sized feldspars that maintains the morphology and features of the original igneous plagioclase, and abundant biotite blades oriented parallel to the main schistosity.

Layer D: fine-grained whitish albitite layer, quite similar to layer B, but with higher phyllosilicate and quartz contents. Thickness is about 20 cm.

Layer E: very thin (a few centimetres) blackish metapelite layer.

Layer F: yellowish layer with a maximum thickness of about 50 cm very similar to layer A.

Layer G: medium- to coarse-grained grey to brown layer about 15 cm-thick showing flattened igneous relict feldspars (30-35 %) up to 5 mm in size oriented parallel to the main schistosity.

Layer B1: very thin layer (2-3 cm) very similar to Layer B.

Layer H: 40-45 cm-thick dark-grey layer containing millimetre-sized and poorly oriented white blastic feldspars. Whitish bands and thin black trails sometimes occur.

A few tens of metres north from the Schina su Enu sequence, a 40-50 cm thick gently folded layer similar to layer G (Figure 3A, B) crops out. This layer, from which sample L81 was collected, consists of a coarse-grained rock very rich in whitish, elongated, millimetre-sized, relict igneous feldspars within a foliated brown matrix. Similar meta-igneous rocks named Lula "porphyroids" by Helbing (2003), consisting of quartz, albite, muscovite/sericite, biotite, chlorite and epidote were described in a neighbouring

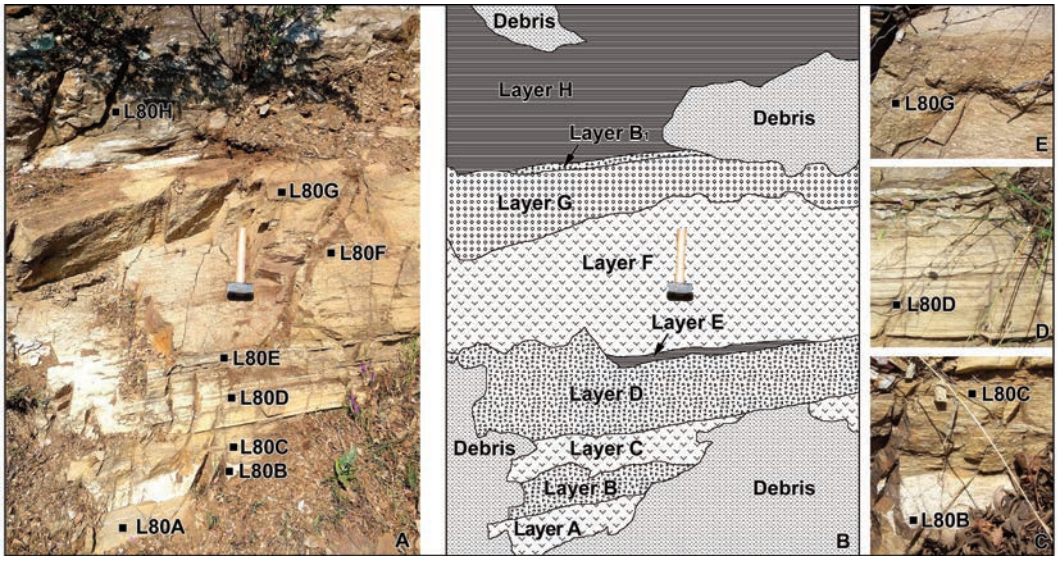

Figure 2. Schina su Enu metavolcanic-sedimentary sequence and close up of the main layers. A) overview of the outcrop; B) drawing of the outcrop; C) close-up of Layers B and C; D) close-up of Layer D with relict plane-parallel laminations; E) close-up of Layer G showing mm-sized phenocrysts of albite and resting unconformably over Layer F.

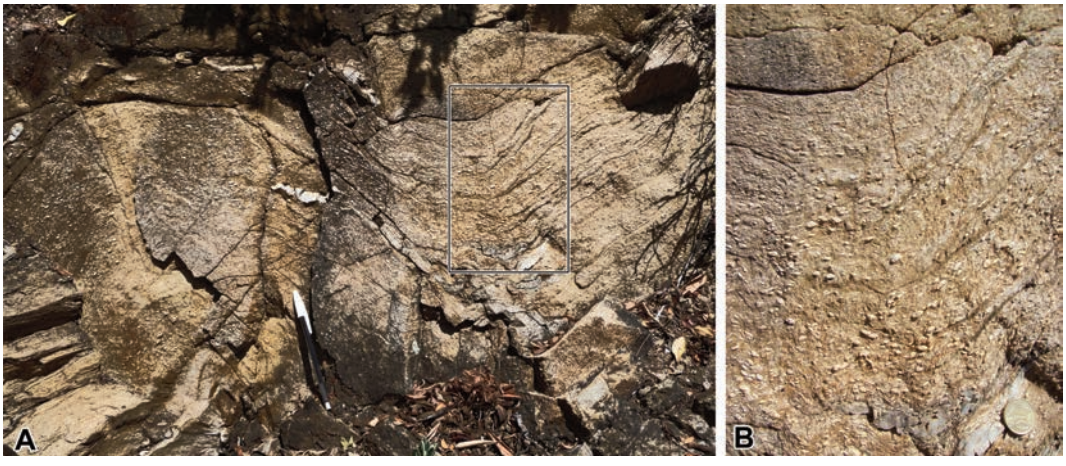

Figure 3. 40-50 cm thick gently folded metavolcanics with variable content of albite phenocrysts a few tens of metres north from the Schina su Enu sequence. A) overview of the outcrop; B) close up of the phenocryst-rich beds.

area. In situ U-Pb zircon dating of these meta-igneous rocks yielded an age of 474 ± 13 Ma (Helbing and Tiepolo, 2005).

The yellowish metasandstone sequences overlying the metavolcanics were studied in a very good exposure (Figures 4, 5) cropping out at Sa Parma approximately 600 m NNE of the Schina su Enu outcrop (Figure 1). The most striking feature of this outcrop is the existence of decametre-sized folds with almost vertical N 40° axial planes. Here, in a 7.5 m-thick stratigraphic section, perpendicular to a fold limb, 45 massive to thinly parallel-laminated short depositional sequences, were analysed in detail. The variable thickness (35 cm to less than 2 cm) of these depositional sequences may be related not only to the single depositional event but also to the degree of tectonic deformation. Sandstone is the main protolith, accompanied by subordinate microconglomerate and siltite. Usually adjacent sequences are separated by a 0.5 to 10 cm-thick dark metapelite layer (Figure 4B). Relict fining-upward grading is locally still recognizable in sandstone layers with an unusual abrupt contact between the uppermost metapelite and the underlying metasandstone layers (Figure 4C). Sometimes the base of the sequence consists of a quartz-rich microconglomeratic layer (Figure 4F) passing upwards to sandstone with an abrupt contact. The contact between the microconglomerate layers at the base of each sequence and the metapelite/metasandstone top of the underlying sequence is abrupt and undulated, resembling an erosion surface. The transition from the yellowish metasandstone layers to the overlying greenish to grey metapsammopelites takes place through alternating metre- to decimetre-sized yellowish and greenish layers or through a gradual decrease of quartz abundance.

The greenish to grey metasedimentary group generally consists of alternating albite rich-phyllites, silver dark phyllites, quartz phyllites, and greenish to gray metapsammopelites. In some outcrops the coarser-grained lithotypes form locally continuous decametre-thick horizons with a gradual transition to the metapelitic (phyllitic) layers. Compared to the yellowish metasandstones, these rocks appear on the whole finer-grained, show a more evident schistosity, a less recognizable original bedding and the appearance of abundant neoblastic albite augen. They also show, in their basal part, decimetre-thick intercalations of yellowish metasandstones. Going towards Lula, the greenish to grey metasedimentary group shows a gradual transition to dark phyllites and schists.

Analytical Methods

The chemical composition of minerals was determined with a fully automated Cameca SX 50 electron microprobe at the Istituto di Geologia Ambientale e Geoingegneria (IGAG-CNR, Roma). Operating conditions were 15 kV accelerating voltage, beam current of 15 nA and 5-10 μm variable spot size. Natural and synthetic wollastonite, olivine, corundum, magnetite, rutile, orthoclase, jadeite, pure Mn, pure Cr, fluorophlogopite and baryte were used as standards. Microstructural study, BSE imaging, and additional EDS chemical analyses were performed using a FEI Quanta 200 SEM equipped with EDAX-EDS detector at the Centro Grandi Strumenti of Cagliari University. Major and trace elements of whole-rock samples were analysed at ALS Minerals Sevilla, Spain.

Petrography

The mineral assemblage and visually estimated mineral modes of selected samples of metavolcanics, yellowish metasandstones, and greenish to grey metapsammopelites are shown in Table 1.

Metavolcanic-sedimentary sequence

As already reported, metavolcanics have been

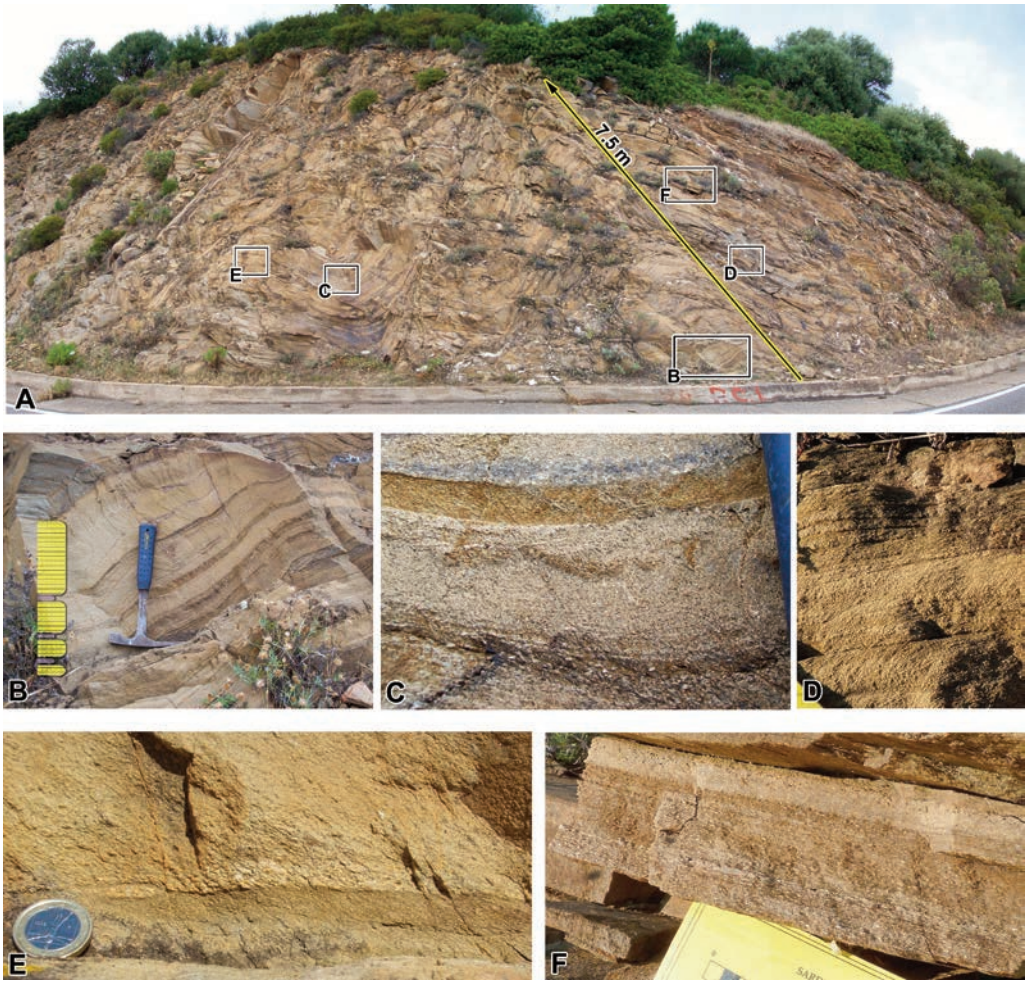

Figure 4. A) Overview of the yellowish metasandstone sequences at Sa Parma showing the location of the enlarged close-ups shown in Fig. 4B, C, D, E, F.; B) Upward-thickening sequence with intercalations of metapelitic layers (sketched on the left); C) Fining-upward sequence from the basal erosion surface to the overlying metapelite layer; D) Plane-parallel laminations in the intermediate part of a sequence (yellow triangle base on the bottom left is 1 cm long); E) Close-up of an erosional contact and basal lag over a metapelitic bed; F) Detail of a microconglomeratic layer passing abruptly upward to sandstone.

identified in a few metre-thick sequence denoted with layer A at the bottom through to layer H at the top.

Layer A - The rock of layer A is made up of quartz, albite, rare oligoclase, K-white mica, biotite, chlorite, epidote, apatite, and Fe-oxides. Worthy of note is the abundance of elongated to subrounded, euhedral to subhedral, unzoned, 4-5 mm-sized albite crystals often including K-white mica, preferentially concentrated in the albite core. The growth of epidote on albite suggests a more calcic composition of the original igneous

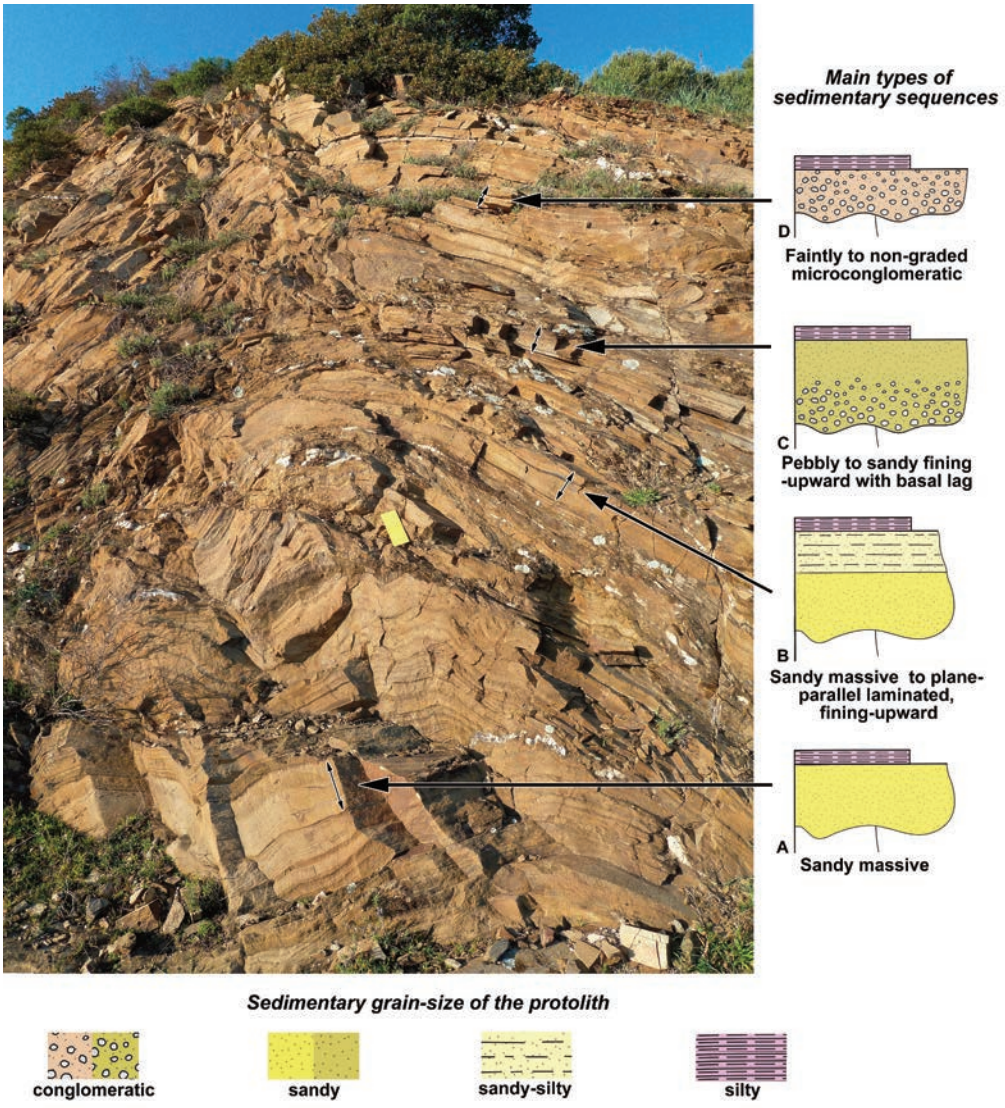

Figure 5. Sa Parma reference sedimentological section and sketches (A, B, C, D) of the main sedimentary sequence types indicated by double arrows. The upper metapelitic bed may sometimes be missing and the subsequent sandy deposit may rest with erosional contact directly on the former sandy sequence. The yellow rectangle for measure is 15 cm long.

plagioclase. Millimetre-sized albite is surrounded by a moderately foliated (S_1) inequigranular matrix consisting of submillimetre- sized quartz, plagioclase, chlorite, K-white mica, biotite and epidote. S_2 crenulation cleavage is also recognizable. Composition of matrix plagioclase varies from albite to oligoclase. Biotite, almost completely chloritised, is by far the less abundant

Table 1. Mineral assemblages and visually estimated mineral modes of selected metavolcanics, albitite, yellowish metasandstones and greenish to grey metapsammopelites from the Lula area. Mineral abbreviation as in Fettes and Desmons (2007).

		Qtz	Pl	Wmca	Chl	Bt	Ep	Grt
Metavolcano-sedimentary sequence	L80A	xx	xx	xx	xx	xx	x	
	L80B	x	xxx	tr	x	tr		
	L80C	xx	xx	xx	tr	xx	tr	
	L80D	xx	xx	xx	tr	x		
	L80G	xx	xx	x	xx	xx	tr	
	L80H	x	xxx	xx	xx	tr	tr	
	L81	xx	xx	tr	xx	xx	tr	
Yellowish metasandstones	L77	xx	xx	xx	xx	x		
	L85	xx	xx	xx	xx	tr	tr	
	L87	xx	xx	x	xx	xx		
	L88	xx	xx	xx	x	xx		
	L90	xx	xx	xx	x	xx		
	L159	xx	xx	xx	xx	xx		
	L161	xx	xx	xx	xx	xx		
	L194	xx	xx	xx	xx	x		
	L196	xx	xx	xx	xx	x		
Metapsammopelites	L67	xx	xx	xx	x	x		
	L78	xx	xx	xx	xx	x		
	L82	xx	xx	xx	xx	tr		
	L83	xx	xx	xx	xx	tr	tr	
	L100	xx	xx	xx	xx	tr		tr
	L103	xx	xx	xx	xx	tr		

xxx > 50 vol.%; 50 vol.% > xx > 5 vol.%; 5 vol.% > x > 1 vol.%; tr: trace amounts or < 1%.

phyllosilicate. K-white mica and chlorite, sometimes associated with minor Fe-oxides, define the main foliation; epidote occurs as small anhedral zoned grains while epidote growing on albite forms small anhedral grains and broad patches with patchy zoning.

Layer B - the rock of layer B (Figure 6A) is a whitish albitite consisting mostly of fine-to-coarse-grained albite (up to 90-95 % modal amount), and minor quartz, chlorite, biotite, apatite, monazite and Fe-oxides. The main feature of this layer is a very fine-grained granoblastic matrix formed by < 50 μm-sized albite grains. Single millimetre-sized albite crystals up to 2-3 mm, with K-white mica overgrowths, were also found. The matrix is characterised by the sporadic occurrence of dark biotite, chlorite, Fe-oxide trails, forming a vague foliation that can be identified as the S_1 schistosity. Quartz only occurs in submillimetre-thick veins or as rare clusters formed by the coalescence of several anhedral grains.

Layer C - the rock of layer C resembles that of Layer A as regards mineralogy and microstructural features, in particular for the occurrence of subrounded to elliptical albite phenocrysts often associated to fine-grained epidote and K-white mica, witnessing the more calcic composition of the original igneous plagioclase. However, compared to Layer A, the rock of Layer C has higher phyllosilicate content, lower abundance of epidote and occurrence of late-crosscutting K-white mica, absent in the rock of Layer A. The S_1 schistosity and a S_2 crenulation cleavage are clearly recognizable. Quartz-filled veins are very common.

Layer D - the rock is very similar to that of Layer B but with larger amounts of phyllosilicate, containing up to 1.5-2.0 mm-sized albite crystals (Figure 6B) rich in fine-grained K- white mica inclusions. The albite crystals are embedded in a mainly quartz-feldspathic matrix made up of albite and < 70-100 μm-sized quartz grains. Albite/quartz ratio in the matrix is

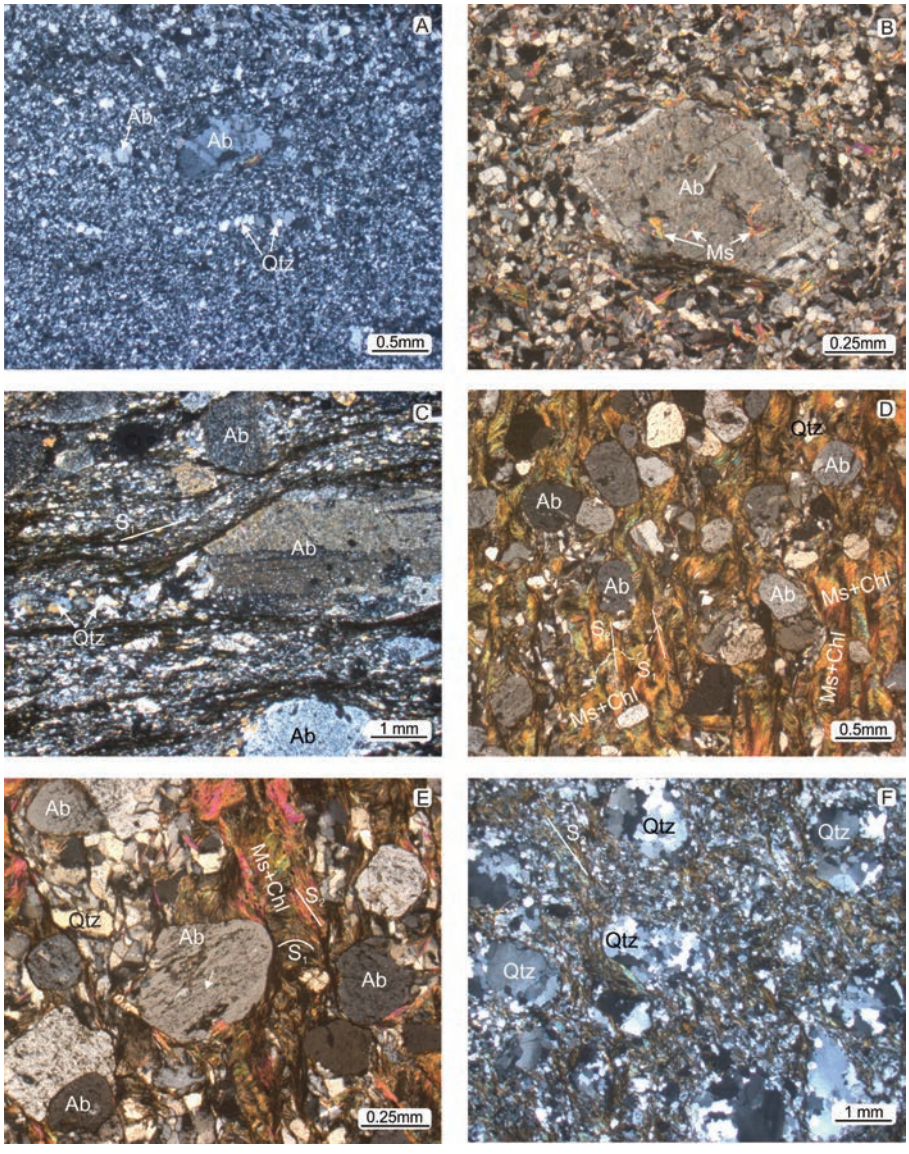

Figure 6. Microstructural features of the metamorphic rocks south of Lula. All photomicrographs are in crossed polars. A) Fine grained albitite Layer (Layer B). In the centre of the photograph a medium-grained albite crystal and a very thin quartz-filled vein can be observed. Sample L80B; B) subhedral albite crystal with white mica overgrowth in a chiefly quartz-feldspathic matrix. Sample L80D; C) metavolcanics from Lula. Note relics of igneous plagioclase phenocrysts, now albite, wrapped around by S_1 schistosity. Sample L80G; D) albite-rich phyllites. S_1 schistosity defined by phyllosilicates is crosscut at high angle by S_2-oriented white mica + chlorite mats. Albite crystals pre-date S_2 schistosity. Sample L80H; E) detail of albite porphyroblasts from sample L80H showing inclusion trails of carbonaceous matter (arrow); F) rounded to elongated pebbles of recrystallised quartz in a microconglomerate sample at the base of a sequence from Sa Parma outcrop. Sample L86.

approximately 1:1. Phyllosilicates in the matrix are mainly K-white mica and biotite. Minor chlorite only occurs as retrograde phase growing on biotite. K-white mica is poorly oriented and evenly distributed throughout the matrix, whereas biotite flakes form biotite clusters. Accessory phases are apatite and Fe-oxides.

Layer E - a very thin, brownish metapelitic Layer.

Layer F - the rock shows the same mineralogy and microstructural features already described for Layer A.

Layer G - the rock is characterised by the occurrence of albite crystals with a maximum size of 2-4 mm in a matrix made up of quartz, albite, chlorite and biotite (Figure 6C). The S_1 schistosity is defined by the alignment of biotite and chlorite blades.

Layer B1 - mineralogical and textural features very similar to those of Layer B.

Layer H - the rock is a brownish albite-rich phyllite characterised by abundant albite porphyroblasts up to 0.7-0.8 mm in size (Figure 6D) with overgrowth of titanite, epidote, chlorite, and apatite. The matrix is composed of small quartz and albite grains and of S_2-oriented K-white mica and chlorite. Phyllosilicatic microlithons preserving a previous S_1 schistosity are often recognizable in the K-white mica+chlorite fringes (Figure 6E). The (quartz + albite)/phyllosilicate ratio of the matrix is strongly variable. Accessory phases are Fe- and Ti-oxides, tourmaline and zircon.

Yellowish metasandstones

Yellowish metasandstones consist of quartz, albite, K-white mica, biotite, chlorite, and minor epidote, apatite, tourmaline, titanite, and Fe-Ti-oxides. Two foliations have been recognised: S_1 is preserved in microlithons whereas S_2, roughly subparallel to the compositional layering, is marked by the alignment of phyllosilicates. Albite crystals occurs as anhedral, flattened, elongated crystals parallel to the main S_2 foliation. Moving northwards, a progressive overprint of the S_2 foliation over the S_1 has been observed. Microconglomerates at Sa Parma (Figure 6F) consist of rounded to elongated pebbles of recrystallised quartz up to 2-2.5 mm in diameter in a moderately foliated matrix made up of quartz, albite, biotite, K-white mica, chlorite, and minor epidote and Fe-Ti oxides. Metapelites interlayered within the yellowish metasandstones show a pervasive S_2 schistosity. Locally S_1-oriented phyllosilicates are preserved in microlithons. These samples are also characterised by the occurrence of medium-grained, late-crosscutting K-white mica. Often the pelite is metapsammopelite resembling those observed in the greenish to grey metasedimentary group or in Layer H. In some layers the albite porphyroblasts may attain 50-60 % percent in volume.

Greenish to grey metapsammopelites

The mineralogical composition of these rocks is: quartz, albite, K-white mica, chlorite, chloritised biotite, and minor epidote, apatite, tourmaline, titanite, and Fe-Ti oxides. Small Mn-rich garnet crystals (MnO ~ 24 wt.%) have been found in sample L100 collected at Schina su Corrale (Figure 1). Two schistosities have been recognised: S_1 and S_2. The S_1 foliation is marked by the alignment of chlorite, K-white mica and subordinate biotite forming short polygonal arcs laterally bounded by the S_2 foliation. The S_2 foliation is sometimes gently folded by the D_3 phase. The distinctive feature of this lithotype is the ubiquitous presence of generally subrounded, sometimes elliptical sub-millimetre to 1-2 mm-sized albite porphyroblasts with the major axis often parallel to the main foliation. They show oriented inclusions of titanite, epidote, apatite, and rare zircon. The albite porphyroblasts are embedded in a lepidoblastic matrix consisting of K-white mica, chlorite and chloritised biotite flakes. Often, layers with high albite/phyllosilicate ratio alternate with layers with lower

albite/phyllosilicate ratio. The thickness of these layers varies from a few millimetres to 1 cm.

Mineral Chemistry

Selected microprobe analyses of biotite, white mica, chlorite, epidote and albite along with the structural formulae are shown in Table 2. All iron is assumed to be divalent iron except for epidote and albite.

Plagioclase. *Albite* is almost pure (Ab > 98 mol %) with CaO content lower than 0.2 wt.% (Ca < 0.01 a.p.f.u.). K_2O content is also very low (K_2O < 0.10 wt.%, K < 0.01 a.p.f.u.). No compositional zoning has ever been detected in albite porphyroblasts. Oligoclase (Ab ~ 77 mol %) has only been found in the matrix of Layer A.

Biotite. Spot analyses often show a low potassium content (K_2O ~ 7-7.5 wt.%) due to widespread chloritisation. Analyses of best preserved biotites show comparable composition between biotites from the yellowish metasandstones (X_{Mg} ~ 0.49) and biotites from the metavolcanics (biotite in Layer A, X_{Mg} ~ 0.51).

White mica. Variable composition. K-white mica from Layer B: Si = 6.88, Na = 0.08 a.p.f.u. and X_{Mg} = 0.62. K-white mica from Layer H: Si = 6.5-6.7; Na = 0.07-0.08 a.p.f.u.; X_{Mg} = 0.49-0.53, showing values similar to those of K-white mica from the yellowish metasandstones (Si = 6.44-6.66; Na = 0.08-0.12 a.p.f.u.; X_{Mg} = 0.46-0.57).

Chlorite shows the following parameters: from Layer A: X_{Mg} = 0.52, Al^{IV} = 2.58 a.p.f.u.; from Layer B: X_{Mg} = 0.47, Al^{IV} = 2.55 a.p.f.u.; from Layer H: X_{Mg} = 0.47, Al^{IV} = 2.49 a.p.f.u.; from yellowish metasandstones: X_{Mg} = 0.48-0.50, Al^{IV} = 2.3-2.5 a.p.f.u..

Epidote yielded the following parameters. From Layer A: X_{Ep} [i.e. $Fe^{3+}/(Fe^{3+} + Al + Cr^{3+} - 2)$] = 0.45- 0.60 and Fe^{3+}_{tot} = 0.45-0.59 a.p.f.u. Layer H: X_{Ep} ~ 0.65 and Fe^{3+}_{tot} ~ 0.60 a.p.f.u.. In the yellowish metasandstones: X_{Ep} = 0.63, Fe^{3+}_{tot} = 0.6 a.p.f.u. to X_{Ep} = 1.05, Fe^{3+}_{tot} = 0.9 a.p.f.u.

P-T conditions

Owing to the absence of the key minerals required for applying conventional thermobarometry, the phase relations and P-T conditions of metamorphism were modelled using the P-T pseudosection approach. For pseudosection modelling, the bulk composition of sample L85 was adopted. This sample shows homogeneous composition, i.e. absence of compositional layering and/or variations. Besides the biotite, chlorite, and white mica do not show significant compositional variations at the thin section scale. A P-T pseudosection has been calculated in the NCKFMASH + Mn + Ti system within the P-T range 370-600 °C, 0.3-1.2 GPa, using Perple_X 6.6.7, following the approach of Connolly (1990) and using the internally consistent thermodynamic dataset and equation of state for H_2O of Holland and Powell (1998, revised 2004). All Fe was assumed to be Fe^{2+} because Fe^{3+}-bearing oxides are absent and epidote is a minor phase. The phases considered in the calculation were biotite, white mica, chlorite, chloritoid, garnet, staurolite, clinopyroxene, amphibole, carpholite, plagioclase, albite, K-feldspar, Al-silicates, lawsonite, zoisite, titanite, rutile, ilmenite, and quartz. Solid solution models are those of Holland and Powell (1998) for garnet, staurolite, and epidote, Powell and Holland (1999) for biotite, Holland et al. (1998) for chlorite, and Fuhrman and Lindsley (1988) for plagioclase. For white mica, the solid solution model by Holland and Powell (1998) has been used together with that of Massonne (2010) in order to distinguish between K-white mica (Wmca1) and Na-white mica (Wmca2). H_2O was considered as a perfectly mobile component and the fluid phase was considered as pure H_2O (aH_2O = 1).

The P-T pseudosection calculated for the composition of sample L85 is shown in Figure 7A. Small variations in aH_2O and Fe^{3+} content slightly changes the width of some multivariant

Table 2. Selected microprobe analyses and structural formulae of biotite, white mica, chlorite, epidote, albite from selected samples of metavolcanite (L80A), albitite (L80B), yellowish metasandstone (L85) and metapsammopelite (L80H) samples.

	L80A	L85	L80B	L80H	L80H	L85	L85	L80A	L80B	L80H	L85	L85	L80A	L80H	L85	L85	L80B	L85
	Bt	Bt	Wmca	Wmca	Wmca	Wmca	Wmca	Chl	Chl	Chl	Chl	Chl	Ep	Ep	Ep	Ep	Ab	Ab
SiO_2	37.18	37.35	50.48	47.60	49.19	47.74	49.51	25.80	25.65	25.69	26.09	25.48	37.05	37.22	37.10	37.05	67.76	67.96
TiO_2	1.54	1.68	0.04	0.33	0.26	0.40	0.29	0.06	0.06	0.05	0.07	0.09	0.12	0.09	0.06	0.07	-	-
Al_2O_3	17.55	16.59	26.87	28.93	27.60	31.60	28.46	21.69	21.61	20.90	19.45	20.61	24.95	24.45	24.49	20.16	18.94	19.14
Cr_2O_3	0.11	0.07	-	-	-	-	0.03	0.06	0.05	0.02	0.07	0.01	0.03	0.02	0.02	-	-	-
FeO*	18.87	19.64	2.93	4.14	3.80	2.78	3.44	24.78	26.42	26.31	25.53	26.60	9.59	10.27	9.85	16.08	-	0.04
MgO	11.01	10.51	2.64	2.19	2.36	1.29	2.56	14.87	13.19	13.22	14.08	13.52	0.09	0.02	0.01	0.01	-	-
MnO	0.12	0.25	0.04	0.03	0.04	-	0.07	0.35	0.31	0.46	0.22	0.33	0.38	0.19	0.28	0.05	-	-
CaO	0.24	0.02	-	0.05	0.09	-	0.04	0.05	0.03	0.07	0.07	0.04	22.48	22.85	22.76	22.53	0.09	0.09
Na_2O	0.09	0.05	0.30	0.25	0.31	0.46	0.29	-	0.02	-	0.01	0.06	-	-	-	-	11.37	11.57
K_2O	9.27	9.71	9.79	9.74	10.12	10.07	10.28	0.07	0.04	0.09	0.31	0.03	-	-	-	-	0.09	0.07
Total	95.98	95.87	93.09	93.26	93.77	94.34	94.97	87.73	87.38	86.81	85.90	86.77	94.69	95.11	94.57	95.95	98.25	98.87
oxygens	22	22	22	22	22	22	22	28	28	28	28	28	12.5	12.5	12.5	12.5	8	8
Si	5.59	5.66	6.88	6.54	6.72	6.44	6.66	5.42	5.45	5.51	5.64	5.47	3.01	3.02	3.02	3.04	3.01	3.00
Al^{IV}	2.41	2.34	1.12	1.46	1.28	1.56	1.34	2.58	2.55	2.49	2.36	2.53	-	-	-	-	0.99	1.00
Al^{VI}	0.70	0.62	3.19	3.23	3.17	3.47	3.18	2.79	2.87	2.80	2.59	2.69	2.39	2.34	2.35	1.95	-	-
Ti	0.17	0.20	0.00	0.03	0.03	0.04	0.03	0.01	0.01	0.01	0.01	0.02	0.01	0.01	0.00	0.00	-	-
Cr	0.01	0.01	-	-	-	-	0.00	0.01	0.01	0.00	0.01	0.00	0.00	0.00	-	-	-	-
Fe^{2+}	2.37	2.49	0.33	0.48	0.43	0.31	0.39	4.35	4.70	4.72	4.61	4.78	-	-	-	-	-	-
Fe^{3+}	-	-	-	-	-	-	-	-	-	-	-	-	0.59	0.63	0.60	0.99	-	0.00
Mg	2.47	2.37	0.54	0.45	0.48	0.26	0.51	4.65	4.18	4.22	4.54	4.33	0.01	0.00	0.00	0.00	-	-
Mn	0.02	0.03	0.01	0.00	0.01	-	0.01	0.06	0.06	0.08	0.04	0.06	0.03	0.01	0.02	0.00	-	-
Ca	0.04	0.00	-	0.01	0.01	-	0.01	0.01	0.01	0.02	0.02	0.01	1.96	1.99	1.99	1.98	0.00	0.00
Na	0.03	0.02	0.08	0.07	0.08	0.12	0.08	-	0.01	-	0.00	0.03	-	-	-	-	0.98	0.99
K	1.78	1.88	1.70	1.71	1.76	1.73	1.77	0.02	0.01	0.03	0.09	0.01	-	-	-	-	0.01	0.00
Total	15.58	15.62	13.85	13.97	13.97	13.93	13.97	19.90	19.84	19.87	19.91	19.92	7.99	7.99	7.99	7.98	4.99	4.99
X_{Mg}	0.51	0.49	0.62	0.49	0.53	0.46	0.57	0.52	0.47	0.47	0.50	0.48						

* : FeOtot in biotite, white mica, chlorite and Fe_2O_3tot in epidote and albite.

fields, leaving the general topology and field assemblages mostly unchanged. The pseudosection is dominated by quadri- (intermediate-grey fields) with minor penta- and tri-variant fields (dark- and light-grey fields, respectively). K-white mica is stable in all the

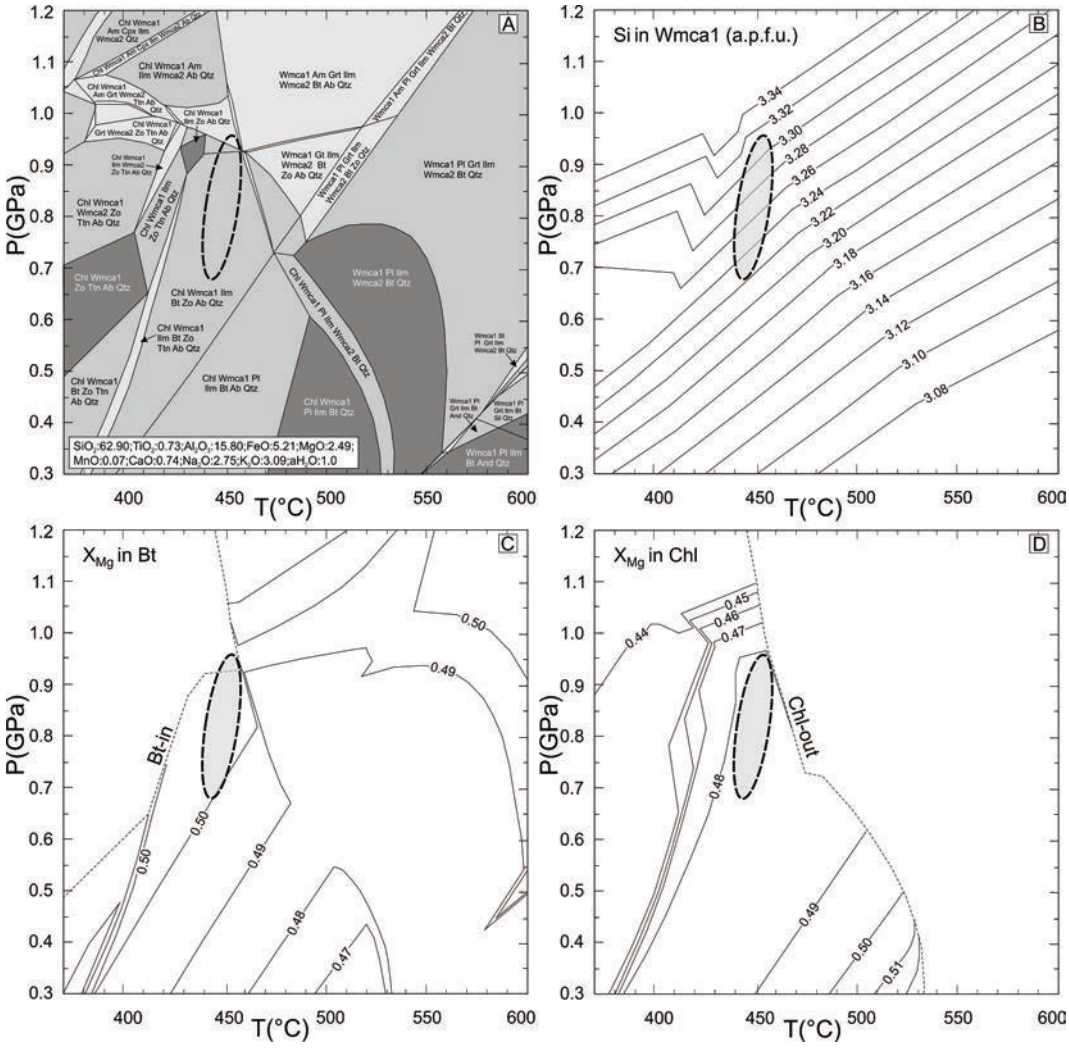

Figure 7. A) P-T pseudosection in the NCKFMASH + Mn + Ti system calculated at a(H_2O) = 1 for the bulk composition of sample L85. White, light-, intermediate- and dark-grey fields are di-, tri-, quadri- and penta-variant fields, respectively. A few small P-T fields are not assigned to a mineral assemblage; B) compositional isopleths for the P-T pseudosection shown in Figure 7a showing variation of Si content in K-white mica; C) compositional isopleths showing variation of X_{Mg} in biotite; D) compositional isopleths showing variation of X_{Mg} in chlorite. Dotted ellipses represent P-T conditions of metamorphism estimated using K-white mica, biotite and chlorite compositional isopleths.

multivariants fields of the P-T pseudosection within the P-T frame considered in the calculation. Biotite entry is roughly between 400 and 450 °C whereas chlorite is stable below 540 °C. The absence of paragonite in the studied samples implies that the P-T conditions of metamorphism did not exceed an upper temperature limit of ~ 460 °C. Further constraints about the P-T conditions can be obtained by comparing the compositional isopleths representing Si (a.p.f.u.) content in K-white mica (Figure 7B), X_{Mg} in biotite (Figure 7C), X_{Mg} in chlorite (Figure 7D) and the actually observed values reported in Table 2 for sample L85. Although small variations in the X_{Mg} values of biotite and chlorite (X_{Mg} = 0.49-0.50, respectively) correspond to wide temperature variations according to the compositional isopleths shown in Figure 7C, D, the observed X_{Mg} ratios and Si content in K- white mica (3.22-3.33 a.p.f.u.) in sample L85 allow to identify an overlapping area in which white mica, chlorite, and biotite are stable within a P-T range of 430-470 °C and 0.65-0.95 GPa (dotted ellipses in Figure 7).

Discussion

Geochemical data obtained on selected samples of metavolcanics, yellowish metasandstones and greenish to grey metapsammopelites are given in Table 3. Owing to intense subsolidus modification of the original magmatic geochemistry a particular attention was paid to immobile elements without neglecting the behaviour of the more mobile elements.

Metavolcanics

The chemical composition of the Lula metavolcanics shows a broad compositional range: SiO_2: 56.2-67.5 wt.%, K_2O: 0.68-3.22, Na_2O: 2.85-5.43, TiO_2: 0.48-0.66, P_2O_5: 0.10-

Table 3. Major element (wt.%) and CIA, trace and rare earth elements (ppm) and Th/U ratio of selected metavolcanics, albitite, yellowish metasandstones and greenish to grey metapsammopelites from Lula area. Samples L100 and L103 are from Schina su Corrale area, samples L194 and L196 from Sos Enattos Mine.

		SiO_2	TiO_2	Al_2O_3	Fe_2O_3	MnO	MgO	CaO	Na_2O	K_2O	P_2O_5	LOI	Total	CIA
Metavolcano-sedimentary sequence	L80A	65.80	0.55	14.75	5.53	0.05	2.55	1.57	4.10	1.06	0.11	3.29	99.50	58
	L80B	67.60	0.07	18.65	0.89	0.02	0.31	0.52	9.60	0.12	0.04	1.21	99.10	53
	L80C	60.20	0.61	17.55	6.15	0.06	2.65	0.94	2.85	3.22	0.12	5.39	99.90	64
	L80D	70.63	0.06	18.23	1.68	0.01	0.37	0.35	4.37	2.64	0.05	1.60	99.99	63
	L80G	56.15	0.66	19.91	8.43	0.13	4.36	0.72	5.43	0.68	0.23	3.28	99.98	64
	L80H	58.60	0.80	18.30	6.99	0.08	2.85	0.52	2.60	3.30	0.20	3.90	98.30	68
Yellowish metasandstones	L81	67.50	0.48	14.35	4.66	0.06	2.32	1.45	4.25	1.05	0.10	3.09	99.40	57
	L77	74.10	0.49	11.65	3.63	0.04	1.30	0.36	3.07	1.55	0.14	2.70	99.10	61
	L85	62.90	0.73	15.80	5.79	0.07	2.49	0.74	2.75	3.09	0.18	2.69	97.40	63
	L87	72.90	0.54	11.75	4.10	0.06	1.32	0.71	3.28	1.50	0.13	2.00	98.40	59
	L88	61.60	0.73	15.85	6.22	0.10	2.49	0.86	2.94	2.79	0.13	4.46	98.30	63
	L90	71.90	0.58	12.70	4.45	0.06	1.71	0.57	3.49	1.35	0.17	2.20	99.20	61
	L159	70.90	0.70	13.50	4.39	0.03	1.30	0.28	2.87	2.31	0.19	2.60	99.20	64
	L161	65.20	0.76	15.20	5.77	0.06	2.15	0.59	2.64	2.42	0.19	3.29	98.40	65
	L194	56.60	0.80	19.65	7.44	0.10	3.10	0.81	2.68	3.68	0.17	4.12	99.30	67
	L196	67.50	0.69	14.40	4.41	0.04	1.60	0.54	4.20	1.40	0.18	2.07	97.20	60
Meta-psammopelite	L67	59.10	0.72	17.50	6.89	0.09	2.77	0.57	2.26	3.35	0.17	4.80	98.30	68
	L78	57.40	0.73	18.75	7.62	0.09	3.33	0.29	1.21	4.43	0.16	4.89	99.00	72
	L82	61.10	0.79	16.40	7.46	0.10	3.60	0.69	1.84	3.09	0.13	3.79	99.10	68
	L83	60.60	0.70	15.80	6.20	0.09	2.69	0.49	2.93	2.57	0.16	3.59	95.90	65
	L100	58.20	0.77	18.95	7.51	0.21	2.05	0.32	1.56	4.05	0.11	3.36	97.20	72
	L103	54.70	0.77	20.40	10.40	0.09	2.39	0.31	1.36	3.36	0.10	4.04	98.00	76

Table 3. Continued ...

		Ba	Rb	Sr	Y	Zr	Nb	Th	Pb	Ga	Zn	Cu	Ni	V	Cr	Hf	Cs	Ta
Metavolcano-sedimentary sequence	L80A	218	59.6	408	15.9	118	5.8	6.63	10	18.2	62	11	23	105	70	3,5	4.10	0.5
	L80B	15	3.1	255	6.9	85	8.7	12.40	9	14.4	13	<5	<5	10	<10	3,9	0.10	0.9
	L80C	865	127.5	292	21.3	175	11.6	10.50	12	25.6	82	<5	22	122	100	5,3	4.02	0.9
	L80D	698	50.4	188	9.9	67	8.4	10.35	<5	19.2	14	<5	<5	<5	<10	3,1	0.60	0.7
	L80G	110	23.8	185	18.4	183	8.3	7.87	7	22.0	66	5	31	108	100	5,2	1.44	0.6
	L80H	696	118.5	115	30.0	176	13.4	12.55	11	26.7	126	30	47	120	90	5,1	3.52	1.0
Yellowish metasandstones	L81	368	45.4	607	14.8	118	7.3	7.11	7	17.9	59	<5	24	89	90	3,6	2.04	0.5
	L77	421	64.9	106	19.0	182	8.8	10.05	17	14.5	69	9	21	53	50	5,3	2.21	0.7
	L85	929	135.0	181	28.9	178	12.3	10.25	9	23.5	114	19	43	101	80	5,0	5.56	1.0
	L87	327	58.6	122	19.2	179	8.8	8.94	11	14.8	71	21	23	61	50	5,0	2.00	0.7
	L88	539	124.5	139	34.3	145	12.7	8.68	24	22.8	131	38	55	97	90	4,4	4.39	1.0
	L90	289	61.9	133	18.3	218	11.5	9.74	15	16.0	78	19	30	76	60	6,1	2.29	0.9
	L159	535	109.5	90	32.5	288	14.2	14.05	10	19.3	59	17	28	85	70	7,7	2.41	1.1
	L161	525	115.0	140	29.2	219	14.3	12.55	20	20.8	101	29	40	109	80	6,2	2.88	1.0
	L194	818	147.0	222	28.9	171	16.7	13.75	23	27.6	269	30	62	143	100	5,0	3.20	1.2
	L196	613	53.8	469	30.5	303	14.3	15.10	7	20.2	65	16	26	95	70	8,6	0.86	1.2
Meta-psammopelite	L67	662	123.5	119	27.2	163	12.2	12.60	12	24.7	134	52	49	110	90	4,8	3.36	0.9
	L78	1005	159.5	90	29.8	142	12.1	12.10	14	28.5	144	34	53	118	90	4,3	4.15	0.9
	L82	672	111.5	89	27.6	157	13.6	13.50	14	23.4	163	73	56	211	100	4,6	3.74	1.1
	L83	528	98.0	121	22.8	159	11.9	10.15	11	22.0	119	30	44	101	80	4,8	3.24	0.9
	L100	938	202.0	168	31.3	148	18.1	16.20	22	28.3	107	<5	49	104	100	4,0	5.44	1.3
	L103	688	202.0	200	34.1	117	16.6	18.20	23	29.5	122	80	40	135	100	3,3	7.86	1.3

		Co	U	La	Ce	Pr	Nd	Sm	Eu	Gd	Tb	Dy	Ho	Er	Tm	Yb	Lu	Th/U
Metavolcano-sedimentary sequence	L80A	12.0	1.53	14.7	22.1	3.38	12.9	2.74	0.84	2.95	0.46	2.76	0.60	1.74	0.26	1.73	0.26	4.3
	L80B	1.8	1.20	23.2	52.6	4.89	17.5	2.91	0.65	2.67	0.31	1.44	0.26	0.76	0.11	0.77	0.12	10.3
	L80C	13.6	2.26	15.7	38.0	3.94	15.6	3.74	0.97	4.32	0.68	4.07	0.81	2.45	0.36	2.41	0.38	4.6
	L80D	0.6	1.25	25.1	43.0	5.29	19.4	3.65	0.64	3.39	0.45	2.15	0.36	0.91	0.11	0.62	0.08	8.3
	L80G	13.9	1.60	20.6	48.1	4.80	17.8	3.78	0.95	4.10	0.60	3.51	0.74	2.13	0.31	2.09	0.32	4.9
	L80H	18.2	2.65	29.6	48.7	6.82	26.5	5.41	1.26	5.76	0.93	5.67	1.19	3.53	0.51	3.39	0.52	4.7
Yellowish metasandstones	L81	14.5	1.79	16.4	35.9	3.95	15.9	3.32	0.80	3.42	0.51	2.82	0.58	1.65	0.24	1.58	0.25	4.0
	L77	7.2	1.67	13.8	27.1	3.59	13.9	2.83	0.69	3.00	0.50	3.25	0.73	2.24	0.34	2.33	0.36	6.0
	L85	17.5	2.61	37.2	66.9	8.46	31.9	6.44	1.38	6.54	0.95	5.43	1.10	3.21	0.46	3.01	0.45	3.9
	L87	9.4	1.63	12.4	41.3	3.13	12.1	2.89	0.76	3.25	0.56	3.57	0.77	2.30	0.35	2.26	0.35	5.5
	L88	21.0	2.41	30.2	65.7	6.78	26.3	5.57	1.33	6.26	0.98	5.82	1.25	3.61	0.52	3.39	0.50	3.6
	L90	7.8	2.35	12.1	24.4	2.91	11.7	2.61	0.62	2.63	0.47	3.08	0.66	1.97	0.32	2.21	0.31	4.1
	L159	9.4	2.16	43.5	82.5	9.40	34.7	7.01	1.34	6.02	0.96	5.64	1.14	3.11	0.47	3.03	0.46	6.5
	L161	16.8	1.78	28.6	49.7	5.50	22.3	4.44	0.96	4.04	0.73	4.72	1.01	2.89	0.45	3.04	0.45	7.1
	L194	16.1	2.96	32.7	43.4	6.79	25.9	5.19	1.18	4.65	0.79	4.96	1.04	3.02	0.48	3.41	0.51	4.6
	L196	11.1	2.82	37.4	78.3	8.87	33.2	6.68	1.14	5.60	0.92	5.57	1.10	3.06	0.49	3.24	0.49	5.4
Meta-psammopelite	L67	14.2	2.67	22.9	45.1	5.69	21.8	4.76	1.10	5.02	0.82	5.09	1.09	3.18	0.47	3.20	0.50	4.7
	L78	21.2	2.36	32.1	65.6	7.34	28.3	5.77	1.30	6.11	0.95	5.56	1.18	3.44	0.49	3.27	0.49	5.1
	L82	17.7	2.38	31.9	58.8	6.92	26.6	5.27	1.16	5.66	0.87	5.21	1.09	3.27	0.48	3.24	0.51	5.7
	L83	17.3	2.05	21.0	48.5	4.92	18.9	4.05	0.93	4.16	0.66	4.25	0.91	2.74	0.41	2.74	0.43	5.0
	L100	21.3	1.65	33.5	56.7	7.02	25.7	4.98	1.07	4.13	0.68	4.37	1.05	3.43	0.55	3.62	0.52	9.8
	L103	17.0	3.03	55.1	49.1	11.65	42.7	8.48	1.76	6.74	1.10	6.35	1.24	3.35	0.51	3.27	0.47	6.0

0.23 (Table 3). In the Nb/Y vs. Zr/TiO_2 diagram (Winchester and Floyd, 1977) the Lula metavolcanics plot at the boundary between the andesite and rhyodacite-dacite fields.

The Lula metavolcanics show significant LREE enrichment, with a steep pattern from sample/chondrite ratios of 10-20 for Eu, up to 60-100 for La, negative Eu anomaly and flat

HREE patterns between 10 and 20 of the sample/chondrite ratio. These patterns are very similar to the Ordovician metavolcanics from Gerrei, Sarcidano and Sarrabus (Giacomini et al., 2006; Gaggero et al., 2012), even if the latter have higher ΣLREE and ΣHREE and a steeper pattern (Figure 8A).

This analogy is confirmed by N-MORB normalised trace element patterns (Figure 8B) (Sun and McDonough, 1989). This diagram demonstrates the calcalkaline affinity of the volcanoclastic materials of the Lula metavolcano-sedimentary sequence. In fact these rocks have the same strong negative anomalies of Nb, Ta, Ti and P that characterise the calcalkaline Middle Ordovician metavolcanics of Gerrei, Sarcidano and Sarrabus (see Memmi et al., 1983; Gaggero et al., 2012). As regards HFSE, the Lula metavolcanics have Ti contents similar to those of the Middle Ordovician metavolcanics but show sometimes substantially lower concentrations of Zr, Y, Nb, Ta and Th. In the Lula metavolcanics we observed a generally strong enrichment in Fe_2O_3, MgO, V, Cr, Co, Ni, Zn compared to the Ordovician metavolcanics from Sarrabus and Gerrei. Interestingly the metavolcanics of the Lula area show almost the same contents in siderophile elements observed in the Ordovician metavolcanics from the Sarcidano, i.e. from the area nearest to the studied outcrops.

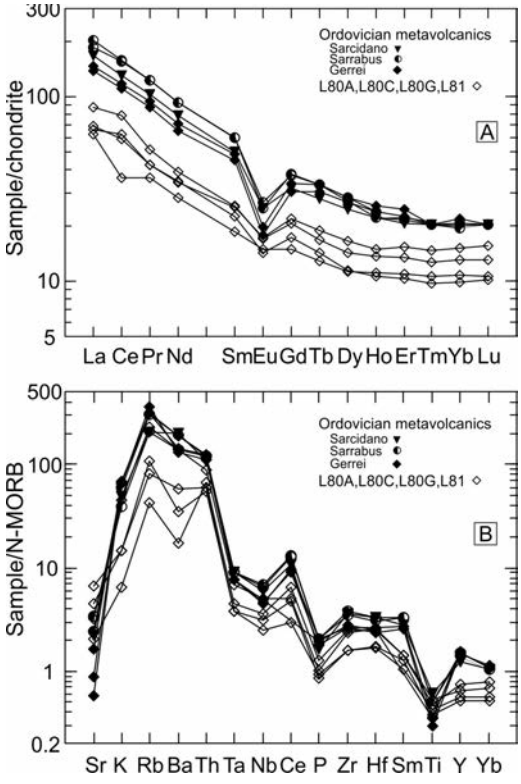

Figure 8. A) Chondrite-normalised REE patterns and (B) N-MORB-normalised spider diagram of L80A, L80C, L80G, and L81 metavolcanics from the Schina su Enu outcrop. The composition of Ordovician metavolcanics from Sarcidano, Sarrabus and Gerrei (from Giacomini et al., 2006) is shown for comparison.

Albitite layers

The discovery of thin (10 cm of thickness) albitite layers in the Lula volcanoclastic metasedimentary sequence is a novelty for the Internal Nappe Zone in Northern Sardinia. Albitites are well known as dykes and small intrusions in Central Sardinia (Castorina et al., 2006 and references therein) and in Sarrabus (SE Sardinia) (see Pirinu et al., 1996 and references therein). The albitites of Lula and particularly the sample L80B show a whole rock composition approaching the almost pure stoichiometric albite. This very anomalous circumstance can be explained only admitting that Na-rich hydrothermal fluids generated the observed albitite layers through a complete metasomatic replacement of volcanoclastic-sedimentary layers or through a lit par lit injection and deposition of hydrothermal albite. The albitisation process could have been generated by the late hydrothermal fluids associated with the Middle Ordovician volcanism (lavas, pyroclastics, ignimbrites) or to late hydrothermal fluids escaping from a Middle Ordovician calcalkaline

intrusive body after enclosed by palingenesis within the Carboniferous Sardinian batholith (see Pirinu et al.,1996; Cavarretta and Puxeddu, 2001; Castorina et al., 2006 and Hövelmann et al., 2010, for a comprehensive bibliography on the albitisation process). The complete lack of albite veins in the studied sequence rules out a late Variscan phenomenon for the albitisation process, associated with the final hydrothermal stages of the underlying Sardinian batholith. This intensive albitisation likely took place during the late hydrothermal activity tied to the Middle Ordovician volcanism testified by the volcanoclastic layers of the Lula sequence. The possible link of the Lula albitites with the Middle Ordovician volcanism offers a unique opportunity to investigate the major and trace element composition of hypothetical late Na-rich hydrothermal fluids connected with the Middle Ordovician volcano-plutonic activity. Taking as a key reference a recent paper by Hövelmann et al. (2010) it is possible to interpret correctly the geochemical data of the Lula rocks. The comparison must be made between sample L80B and the not metasomatised samples L80A, L80C, L80G and L80H; each of these samples could represent the possible not albitised protolith. Similarly to what observed by Hövelmann et al. (2010, Figure 4) for gains and losses of elements during an albitisation process the sample L80B shows remarkable losses of TiO_2 , Fe_2O_3, MgO, K_2O, Zn, Ni, V, Sr, HREE and extremely high losses of Ba and Rb. On the contrary the sample L80B is characterised by slight gains of Th and LREE from La to Sm. The enrichment in LREE and depletion in HREE in the Lula albitites is not surprising and very similar to what observed in albitites of Central Sardinia by Bornioli et al. (1997). The gains and losses of elements in L80B suggest modification of the protolith chemistry through replacement of biotite and Ca-plagioclase, while sample L80D, that does not show losses in K_2O, Ba, Rb, but mainly in CaO, underwent albitisation of only Ca-plagioclase.

Provenance of sedimentary materials of yellowish metasandstones and greenish to grey metapsammopelites

In the K_2O/Na_2O vs. SiO_2/Al_2O_3 diagram (Figure 9, Wimmenauer, 1984) the yellowish metasandstones plot in the greywacke field, with a few samples in the pelitic greywackes field. The greenish to grey metapsammopelites plot in both the pelites and pelitic greywackes fields. Sample L80H at the top of the metavolcano-sedimentary sequence plots in the field of pelitic greywacke. For the provenance of detrital materials of the metasandstones and metapsammopelites we consider again the chondrite normalised REE patterns (Figure 10A). The REE patterns of the metapsammopelites are almost identical to the Ordovician metavolcanics from the Sarcidano, Sarrabus and Gerrei (Figure 8A) and to those of NASC (North American Shale Composite) and PAAS (Post Archaean Australian Shales) (Figure 10A) and resemble the patterns of pelites from the Rautgara Formation, Kumaun Lesser Himalaya (Rashid, 2005, Figure 1) and of Sillakkudi sandstones, southern India (Bakkiaraj et al., 2010, Figure 4). The metasandstones show similar patterns apart from a group of samples

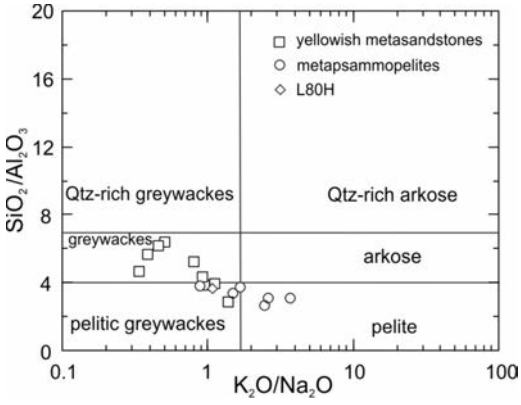

Figure 9. Geochemical composition of the yellowish metasandstones, metapsammopelites and sample L80H in the K_2O/Na_2O vs. SiO_2/Al_2O_3 classificative diagram after Wimmenauer (1984).

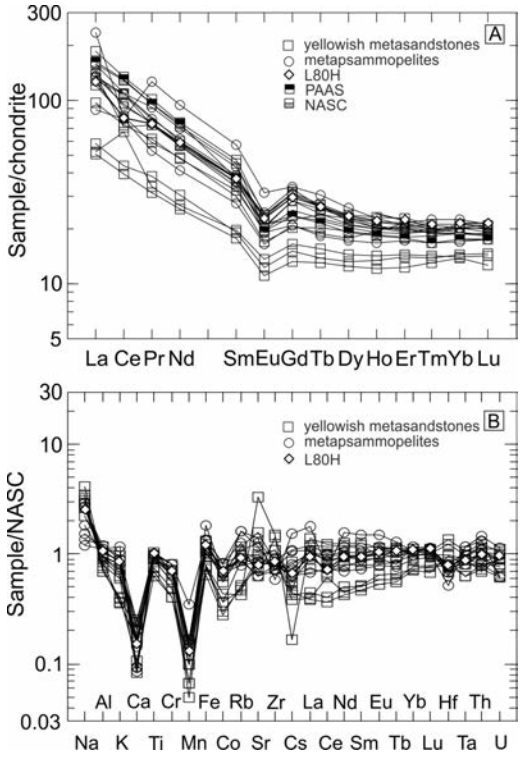

Figure 10. A) Chondrite-normalised REE patterns and (B) North American Shale Composite (NASC)-normalised spider diagram of yellowish metasandstones, metapsammopelites and sample L80H from Lula area.

displaying less pronounced LREE enrichment, less evident negative Eu anomalies and lower ΣLREE and ΣHREE than the Sardinian Ordovician metavolcanics, NASC, and PAAS. The metasandstones closely resemble the patterns of the Lula metavolcanics. According to Rashid (2005, p. 1835) "the significant enrichment of LREEs, the distinctive negative Eu-anomalies and the flat HREE patterns ... suggest derivation from an old upper continental crust composed chiefly of felsic components". These features seem to indicate that the source rocks of the Lula metasediments were the older Precambrian to early Paleozoic felsic igneous to metamorphic rocks outcropping in NE Sardinia. Other interesting features are revealed by Figure 10b showing the depletion and enrichment in major and trace elements of metasandstones and metapsammopelites with respect to North American Shale Composite (NASC). The Lula rocks appear remarkably enriched in Na_2O, strongly depleted in CaO, MnO, slightly depleted in Al_2O_3, K_2O, TiO_2, Cr, Co and REE. This behaviour seems to indicates that hydrothermal processes similar to those that produced the albitites could have partially interested also the metasandstones and the metapsammopelites, with the consequent alteration of Ca-plagioclase, and biotite. A continental margin provenance is suggested by the Th-Co-Zr/10 (Bhatia and Crook, 1986) diagram (Figure 11) in which most of the Lula samples plot in the B field (continental island arc) a few samples fall in the C field (active continental margin) and few samples plot in an intermediate position between B and C fields and the Co apex, but with relative abundance of Th significantly higher than in the A field (ocean island arc). These results confirm that the sedimentary materials were supplied by dismantling of an older active continental margin or island arc.

Intensity of weathering and oxidizing conditions of the sedimentary environment

The geochemical data give useful information about the degree of alteration of the rocks supplying the sedimentary material, the oxidizing or reducing conditions of the original sedimentary environment and the nature of the source rocks from which the metasediments derived. A useful tool to evaluate the degree of weathering is the chemical index of alteration (CIA, Nesbitt and Young, 1982) that can be obtained calculating the formula (molecular proportion):

$$CIA = [Al_2O_3/(Al_2O_3 + CaO^* + Na_2O + K_2O)] \times 100$$

where CaO* is the amount of CaO

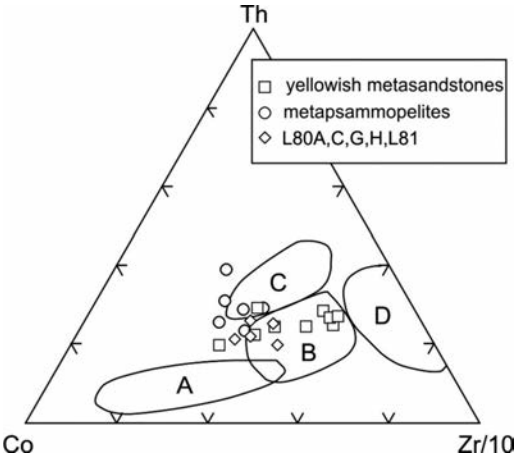

Figure 11. Th-Co-Zr/10 classification diagram for the Lula samples. A: ocean island arc, B: continental island arc, C: active continental margin, D: passive continental margin (Bhatia and Crook, 1986) .

incorporated in the silicate fraction of the rock. However considering that the CaO content of the Lula rocks is very low (in 18 samples out of 22 CaO is lower than 0.9 and in several samples lower than 0.5) and carbonates were never observed in the Lula rocks, all the CaO has been assumed to be incorporated in silicates (see Nagarajan et al., 2007, page 304, for a more detailed discussion).

The CIA values for almost all the studied Lula rocks (Table 3) are intermediate between those typical of no alteration (CIA < 50) and those indicating intensive alteration (CIA > 70). The greenish to grey metapsammopelites are characterised by CIA values in the range 65-76 that could be explained by larger amounts of the clay fraction or by a more pronounced alteration of the source rocks. The yellowish metasandstones yielding CIA values in the range 59-67 include more frequent sand-rich layers or received less weathered sedimentary materials compared to the metapsammopelites. The different behaviour of the two lithotypes is confirmed by the A-CN-K diagram (Nesbitt and Young, 1982) (Figure 12). This diagram shows a gradual transition of the Lula samples from the metavolcanics, close to the feldspar join and to the A-CN side, to the metapsammopelites, near to or coincident with the average shale field (dashed rectangle in Figure 12), as defined by Rashid (2005, Figure 2) and close to the opposite A-K side. A very similar trend from A-CN side towards higher values of K component just near the A-K side was hypothesized by Barbera et al. (2006), for the Soro shales in Sicily, as a weathering trend from the source rocks. This means increasing weathering intensity of the source rocks or increasing content of the clay component from the metavolcanics and yellowish metasandstones to the metapsammopelites, confirming the information provided by the CIA values.

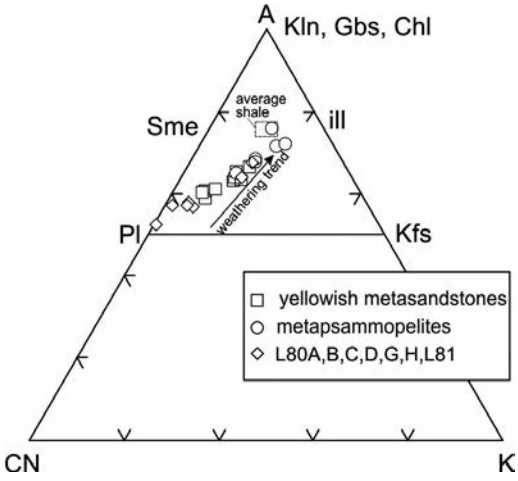

Figure 12. Composition of the Lula samples in the A-CN-K diagram after Nesbitt and Young (1982). The plagioclase-K-feldspar join, as well as the composition of smectite, illite, kaolinite, gibbsite and chlorite are shown for comparison. Dashed rectangle represents the composition of average shale as defined by Rashid (2005).

Another interesting parameter is the Th/U ratio (Table 3). The increasing intensity of weathering from the metavolcanics to the other two lithotypes is clearly depicted in a Th vs. Th/U diagram (McLennan et al., 1993) (not shown here). Bakkiaraj et al. (2010, Figure 6) have shown that the samples of Sillakkudi sandstones from southern India plot along a weathering trend that produces a significant and gradual increase of the Th/U ratio from values of 4-5 for the fresh samples to the highest values of 16-20 yielded by the most weathered samples. The plot in Figure 6 of Bakkiaraj et al. (2010) clearly demonstrates that the weathering process starts for values higher than Th/U ratio of 6-7. The Lula metasedimentary samples follow a similar trend: metapsammopelite samples have Th/U values in the range 4.7-9.8, 5 out of 9 yellowish metasandstone samples fall in the range 5.4-7.1, while all the metavolcanic samples, except for the albitite samples, show values lower than 4.9.

The different proportions of the sandy and clayey components in the metasandstones and metapsammopelites clearly emerge from the geochemical comparison of the two lithotypes. Compared to the metapsammopelites, the metasandstones reveal slightly higher contents in SiO_2, Zr and Hf, strong enrichment in Na_2O, slightly lower Al_2O_3, Fe_2O_3, Ba, Rb and Cs contents, and strong depletion in K_2O. Both groups show very similar contents for all the other major and trace elements. These differences suggest that the metasandstones are composed chiefly of a sandy component rich in detrital heavy minerals. In this comparison, on the contrary, the metapsammopelites show larger amounts of K- and Al-rich clay minerals.

Several geochemical parameters suggest that the sedimentary environment was characterised by prevailing oxidizing conditions for both groups of metasediments and also for the metavolcanics, in the case of reworking. According to Nagarajan et al. (2007), who take into account the study by Nath et al. (1997), U/Th < 1.25, V/Cr < 2, Ni/Co < 5 and Cu/Zn in the range 0.08-0.66 indicate oxidizing conditions. All the Lula rocks have U/Th in the range 0.10-0.28, V/Cr in the range 0.99-1.50 (except sample L82 with 2.11), Ni/Co in the range 1.62-3.85, Cu/Zn in the range 0.11-0.66. Oxidizing environment, according to Rashid (2005), produces high ΣREE and negative Eu anomalies: both these features characterise the Lula samples. The only ambiguous feature is the negative Eu anomaly that could be produced by early fractionation of plagioclase. However this possible alternative interpretation can be excluded because most of the Lula rocks are not true metavolcanics but metasediments only enriched in volcanoclastic material, as suggested by their mineralogical composition.

Paleoenvironmental features of the metavolcanic and metasedimentary sequences

Many of the original volcanic and sedimentary features in the Lula area were erased or hindered by the Variscan metamorphism. Therefore it is very difficult to reconstruct paleoenvironments of the Lula rocks. However, some residual volcanic and sedimentary structures still survive in low-strain areas spared by the tectonic deformations. The shallow metavolcanic succession of Schina su Enu probably consists of primary volcanic products and/or deposits of their reworked materials. Thin, discontinuous dark metapelitic layers in the middle (layer E) and at the top (layer H) of the metavolcanic succession could represent true sedimentary layers marking short quiescence periods in the volcanic activity. The metasedimentary rocks may be referred to shallow marine sediments: the protolith of the yellowish metasandstones shows features of mid- to subordinately high-energy environment while that of the metapsammopelite succession may be referred to alternating mid- and more common low-energy environments. The relict sedimentary structures and the architecture of the sequences indicate massive to

tractional-type depositional processes with a variety of intermediate cases. The occurrence of the interlayered metapelitic beds indicates that clay settled in low-energy depositional environments. In the yellowish metasandstones some relict sedimentary trends, such as the thickening- to thinning-upwards of the forty-five observed sequences, may be tentatively interpreted as a backward to forward migration of the sequences with respect to the shoreline, reflecting increasing to decreasing mean depositional energy, respectively. Conversely, in the metapsammopelites coarse-grained deposits such as conglomerates are missing altogether, while complete depositional sequences are characterised by very small thickness, finer-grained sediments and an erratic distribution, suggesting a quieter, steady environment, typical of prevailing low-energy environment in contraposition to the more dynamic prevalently mid-energy environment previously described for the yellowish metasandstones. The whole succession from the metavolcanics to the metapsammopelites was deposited in variable environments from shallow marine environments for metavolcanics and from shallow to mid-shelf marine environments for yellowish metasandstones, metapsammopelites and blackish metapelites.

A correlation of the Lula sequences with the better known stratigraphic units of the Nappe Zone can be tentatively proposed. The metavolcanics recall the Ordovician "orogenic" magmatic complex cropping out in all the Variscan successions of Sardinia. The yellowish metasandstones are similar to the post-volcanic Late Ordovician complex formed by the Punta Serpeddì, Genna Mesa Metarkoses and Orroeledu Formations of the Sarrabus, Gerrei and Meana Sardo of the External Nappe Zone (Carmignani et al., 2001, and references therein).

Concluding remarks

This is the first attempt to identify, in greater detail, the geochemical and petrographical features of the metavolcano-sedimentary sequences of NE Sardinia. In the Lula area, NE Sardinia, a metavolcano-sedimentary sequence of possible Middle Ordovician age, including pure albitite layers (albite up to 90- 95 % modal content, Na_2O up to 9.60 wt.%) has been discovered. Three main lithotypes have been identified from bottom to top: 1) metavolcanics; 2) yellowish metasandstones; 3) greenish to grey metapsammopelites. The metavolcanics and the overlying metasedimentary rocks are very similar to the Ordovician metavolcano-sedimentary sequences of central and southern Sardinia.

The metavolcanics show a compositional range between andesite and rhyodacite-dacite. They are characterised by a steep LREE enrichment pattern, negative Eu anomaly and flat HREE patterns. The Ordovician metavolcanics from Gerrei, Sarcidano and Sarrabus, including typical calcalkaline lithotypes such as andesites and dacites show patterns for all the immobile elements that closely resemble those of the metavolcano-sedimentary layers of the Lula area. The N-MORB-normalised trace element patterns demonstrate the calcalkaline affinity of the Lula metavolcanics, as indicated by negative anomalies of Ta, Nb, Ti and P.

As regards the provenance of detrital materials, the metapsammopelites and the metasandstones are almost identical to those of the Ordovician metavolcano-sedimentary sequences from Gerrei, Sarcidano and Sarrabus and to those of NASC and PAAS. The protolith of the Lula samples were sediments deposited in shallow marine to mid-shelf environments and rich in volcanoclastic material supplied by the dismantling of volcanics typical of an active continental margin. The CIA values of the Lula samples vary from those typical of weakly weathered rock with two values out of four lower

than 60 for the metavolcanics and a continuous transition from low to strong alteration (CIA = 59-76) for metasandstones and metapsammopelites.

The great novelty of the Lula sequence is the occurrence of almost pure albitite layers generated by Na metasomatism. The rocks were metamorphosed and multideformed during the Variscan orogeny. Geothermobarometry with pseudosection modelling on a metasandstone sample from the biotite zone gives T = 430-470 °C and P = 0.65-0.95 GPa.

Acknowledgements

The authors would like to thank M. Serracino (IGAG-CNR Roma) for assistance with the electron microprobe. The authors are also grateful to Patrizia Fiannacca (Università di Catania) and an anonymous reviewer for their helpful comments. This research was supported by a MIUR-PRIN 2008 grant awarded to M. Franceschelli.

References

Bakkiaraj D., Nagendra R., Nagarajan R. and Armstrong-Altrin J.S. (2010) - Geochemistry of sandstones from the Upper Cretaceous Sillakkudi Formation, Cauvery Basin, southern India: Implication for provenance. *Journal of the Geological Society of India*, 76, 453-467.

Barbera G., Mazzoleni P., Critelli S., Pappalardo A., Lo Giudice A. and Cirrincione R. (2006) - Provenance of shales and sedimentary history of the Monte Soro Unit, Sicily. *Periodico di Mineralogia*, 75, 313-330.

Bhatia M.R. and Crook K.A.W. (1986) - Trace element characteristics of graywackes and tectonic setting discrimination of sedimentary basins. *Contributions to Mineralogy and Petrology*, 92, 181-193.

Bechstadt T. and Boni M. (1994) - Sedimentological, stratigraphical and ore deposits field guide of the autochthonous Cambro-Ordovician of Southwestern Sardinia. Servizio Geologico d'Italia, 434 pp.

Bornioli R., Carcangiu G., Palomba M., Simeone R. and Tamanini M. (1997) - Rare earth elements in the Albitites of Central Sardinia (Italy). Note I: The mineralization of Ottana. *Periodico di Mineralogia*, 66, 269-285.

Calvino F., Dieni I., Ferasin F. and Piccoli G. (1958) - Rilevamento geologico della parte meridionale del foglio n°195 Orosei. *Bollettino della Società Geologica Italiana*, LXXVII.

Carmignani L., Franceschelli M.,Ghezzo C.,Gattiglio M., Pertusati P.C. and Ricci C.A. (1982) - Attuali conoscenze sul ciclo ercinico nella Sardegna Settentrionale. In: Guida alla Geologia del Paleozoico sardo. Guide Geologiche Regionali. Società Geologica Italiana, 129-135.

Carmignani L., Conti P., Pertusati P.C., Barca S., Cerbai N., Eltrudis A., Funedda A., Oggiano G. and Patta D. (2002) - Note Illustrative della Carta Geologica d'Italia alla scala 1:50.000, Foglio 549 Muravera. Servizio Geologico d'Italia, pp. 140, L.A.C., Firenze.

Carmignani L., Oggiano G., Barca S., Conti P., Eltrudis A., Funedda A., Pasci S. and Salvadori I. (2001) - Geologia della Sardegna (Note illustrative della Carta Geologica della Sardegna in scala 1:200.000). Memorie descrittive della Carta Geologica d'Italia, Servizio Geologico Nazionale. Istituto Poligrafico e Zecca dello Stato, Roma.

Carosi R. and Palmeri R. (2002) - Orogen-parallel tectonic transport in the Variscan belt of northeastern Sardinia (Italy): implications for the exhumation of medium-pressure metamorphic rocks. *Geological Magazine,* 139, 497-511.

Castorina F., Masi U., Padalino G. and Palomba M. (2006) - Constrains from geochemistry and Sr-Nd isotopes for the origin of albitite deposits from Central Sardinia (Italy). *Mineralium deposita*, 41, 323-338.

Cavarretta G. and Puxeddu M. (2001) - Two-mica F-Li-B-rich monzogranite apophysis of the Larderello Batholith cored from 3.5km depth. *Neues Jahrbuch für Mineralogie Abhandlungen*, 177, 77-112.

Connolly J.A.D. (1990) - Multivariable phase diagrams: an algorithm based on generalized thermodynamics. *American Journal of Science*, 290, 666-718.

Di Vincenzo G., Carosi R. and Palmeri R. (2004) - The Relationship between tectono-metamorphic evolution and argon isotope records in white mica: constraints from in situ ^{40}Ar-^{39}Ar laser analysis of the Variscan basement of Sardinia. *Journal of*

Petrology, 45, 1013-1043.

Elter F.M., Franceschelli M., Ghezzo C., Memmi I. and Ricci C.A. (1986) - The geology of northern Sardinia. In: Carmignani L., Cocozza T., Ghezzo C., Pertusati P.C., Ricca C.A., (Eds.) Guide-book to the excursion on the paleozoic basement of Sardinia. IGCP Project No. 5, Newsletter, special issue, 87-102.

Elter F.M., Faure M., Ghezzo C. and Corsi B. (1999) - Late Hercynian shear zones in northeastern Sardinia (Italy). *Géologie de la France,* 2, 3-16.

Elter F.M., Musumeci G. and Pertusati P.C. (1990) - Late Hercynian shear zones in Sardinia. *Tectonophysics,* 176, 387-404.

Fettes D. and Desmons J. (Eds) (2007) - Metamorphic Rocks: a classification and glossary of terms. Recommendations of the international union of geological science Subcommission on the systematic of metamorphic rocks. Cambridge University Press. Cambridge UK, 244 p.

Franceschelli M., Memmi I. and Ricci C.A. (1982) - Zoneografia metamorfica della Sardegna settentrionale. Guida alla Geologia del Paleozoico sardo. Guide Geologiche Regionali, Società Geologica Italiana, 137-149.

Franceschelli M., Memmi I., Pannuti F. and Ricci C.A. (1989) - Diachronous metamorphic equilibria in the Hercynian basement of northern Sardinia, Italy. In: Daly J.S., Cliff R.A. and Yardley B.W.D. (eds) Evolution of metamorphic belts. Geological Society of London Special Publication, 43, 371-375.

Franceschelli M., Puxeddu M. and Cruciani G. (2005) - Variscan metamorphism in Sardinia, Italy: review and discussion. In: (eds.) Carosi R., Dias R., Iacopini D., and Rosenbaum G., The southern Variscan belt, *Journal of the Virtual Explorer*, Electronic Edition, Volume 19, Paper 2.

Fuhrman M. and Lindsley D. (1988) - Ternary-feldspar modeling and thermometry. *American Mineralogist*, 73, 201-215.

Gaggero L., Oggiano G., Funedda A. and Buzzi L. (2012) - Rifting and arc-related early Paleozoic volcanism along the north Gondwana margin: geochemical and geological evidence from Sardinia (Italy). *Journal of Geology*, 120, 273-292.

Giacomini F., Bomparola R.M. and Ghezzo C. (2005) - Petrology and geochronology of metabasites with eclogite facies relics from NE Sardinia: constraints for the Palaeozoic evolution of Southern Europe. *Lithos*, 82, 221-248.

Giacomini F., Bomparola R.M., Ghezzo C. and Guldbransen H. (2006) - The geodynamic evolution of the Southern European Variscides: constraints from the U/Pb geochronology and geochemistry of the Lower Palaeozoic magmatic-sedimentary sequences of Sardinia (Italy). *Contributions to Mineralogy and Petrology*, 152, 19-42.

Helbing H. (2003) - No suture in the Sardinian Variscides: A structural, petrological, and geochronolgical analysis. Tubinger Geowissenshaftliche Arbeiten, Reihe A 68, 1-190.

Helbing H. and Tiepolo M. (2005) - Age determination of Ordovician magmatism in NE Sardinia and its bearing on Variscan basement evolution. *Journal of the Geological Society of London*, 162, 689-700.

Holland T., Baker J. and Powell R. (1998) - Mixing properties and activity-composition relationships of chlorites in the system MgO-FeO-Al_2O_3-SiO_2-H_2O. *European Journal of Mineralogy*, 10, 395-406.

Holland T.J.B. and Powell R. (1998) - An internally consistent thermodynamic data set for phases of petrologic interest: *Journal of Metamorphic Geology*, 16, 309-343.

Hövelmann J., Putnis A., Geisler T., Schmidt B.C. and Golla-Schindler U. (2010) - The replacement of plagioclase feldspars by albite: observations from hydrothermal experiments. *Contributions to Mineralogy and Petrology*, 159, 43-59.

Leone F., Hamman W., Laske R., Serpagli E. and Villas E. (1991) - Lithostratigraphic units and biostratigragraphy of the post-sardic Ordovician sequence in south-west Sardinia. *Bollettino della Società Paleontologica Italiana*, 30, 2, 201-235.

Massonne H.-J. (2010) - Phase relations and dehydration behaviour of calcareous sediments at very-low to low grade metamorphic conditions. *Periodico di Mineralogia*, 79, 21-43.

McLennan S.M., Hemming S., McDaniel D.K. and Hanson G.N. (1993) - Geochemical approaches to sedimentation, provenance, and tectonics. In : M.J. Johnson and A. Basu (Eds), Processes Controlling the Composition of Clastic Sediments. *Geological Society of America Special Paper*, 284, 21-40.

Memmi I., Barca S., Carmignani L., Cocozza T., Franceschelli M., Gattiglio M., Ghezzo C., Minzoni N., Naud G., Pertusati P.C. and Ricci C.A. (1983) - Il magmatismo pre-ercinico della Sardegna, In:

(Eds) Carmignani L., Cocozza T., Ghezzo C., Pertusati P.C., Ricci C.A. - Guida alla Geologia del Paleozoico Sardo, pp. 157-164.

Nagarajan R., Madhavaraju J., Nagendra R., Armstrong-Altrin J.S. and Moutte J. (2007) - Geochemistry of Neoproterozoic shales of the Rabanpalli Formation, Bhima Basin, Northern Karnataka, southern India: implications for provenance and paleoredox conditions. *Revista Mexicana de Ciencias Geologicas*, 24, 150-160.

Nath B.N., Bau M., Ramalingeswara Rao B. and Rao Ch.M. (1997) - Trace and rare earth elemental variations in Arabian Sea sediments through a transect across the oxygen minimum zone. *Geochimica et Cosmochimica Acta*, 61, 2375-2388.

Nesbitt H.W. and Young Y.M. (1982) - Early Proterozoic climate and plate motions inferred from major element chemistry of lutites. *Nature*, 299, 715-717.

Oggiano G. and Di Pisa A. (1992) - Geologia della catena Ercinica in Sardegna-Zona Assiale. In: Carmignani L., Pertusati P.C., Barca S., Carosi R., Di Pisa A., Gattiglio M., Musumeci G., Oggiano G. (Eds), Struttura della catena ercinica in Sardegna. Guida all'escursione. Gruppo Informale di Geologia Strutturale, 147-177, Siena.

Oggiano G., Gaggero L., Funedda A., Buzzi L. and Tiepolo M. (2010) - Multiple early Paleozoic volcanic events at the northern Gondwana margin: U-Pb age evidence from the Southern Variscan branch (Sardinia, Italy). *Gondwana Research*, 17, 44-58.

Padovano M., Elter F.M., Pandeli E. and Franceschelli M. (2012) - The East Variscan shear zone: new insights into its role in the Late Carboniferous collision in southern Europe. *International Geology Review,* 54, 957-970.

Pertusati P.C., Sarria E., Cherchi G.P., Carmignani L., Barca S., Benedetti M., Chighine G., Cincotti F., Oggiano G., Ulzega A., Orrù P. and Pintus C. (2002) - Note Illustrative della Carta Geologica d'Italia alla scala 1:50.000, Foglio 541 Jerzu. Servizio Geologico d'Italia, pp. 169, L.A.C., Firenze.

Pirinu N., Brotzu P., Callegari E. and Secchi F. (1996) - Age and field relationships of albite-rich monzosyenite intruded into the Sarrabus granitoids (SE Sardinia, Italy). *Periodico di Mineralogia*, 65, 289-304.

Powell R. and Holland T. (1999) - Relating formulations of the thermodynamics of mineral solid solutions: activity modeling of pyroxenes, amphiboles and micas. *American Mineralogist*, 84, 1-14.

Rashid S.A. (2005) - The Geochemistry of Mesoproterozoic clastic sedimentary rocks from the Rautgara Formation, Kumaun Lesser Himalaya: implications for provenance, mineralogical control and weathering. *Current Science*, 88, 1832-1836.

Sun S.S. and McDonough W.F. (1989) - Chemical and isotopic systematics of oceanic basalts: implications for mantle composition and processes. In: Saunders AD, Norry MJ (eds) Magmatism in the ocean basins. Geological Society, London, pp. 313-345.

Wimmenauer W. - (1984) Das praevariszische Kristallin im Schwarzwald. Forscht Miner Beih, 62, 69-86.

Winchester J.A. and Floyd P.A. (1977) - Geochemical discrimination of different magma series and their differentiation products using immobile elements. *Chemical Geology*, 20, 325-343.

Submitted, March 2012 - Accepted, July 2012